

Baldwin Samuel N (Orcid ID: 0000-0002-3796-6090)  
Andrew Ruth (Orcid ID: 0000-0002-6916-2994)  
Isakson Brant E. (Orcid ID: 0000-0002-7692-6294)  
Greenwood Iain A (Orcid ID: 0000-0002-0603-0492)

Marked oestrus cycle-dependent regulation of rat arterial Kv7.4 channels driven by  
GPER1

GPER1 regulation of arterial Kv7.4

Samuel N Baldwin BSc (Hons), Elizabeth A. Forrester (BSc), Natalie ZM Homer<sup>1</sup>  
(PhD), Ruth Andrew<sup>1, 2</sup> (PhD) Vincenzo Barrese<sup>3</sup> (MD, PhD), Jennifer B Stott (PhD),  
Brant E. Isakson<sup>4</sup> (PhD), Anthony P Albert (PhD), Iain A Greenwood (PhD)

Vascular Biology Research Centre, Institute of Molecular and Clinical Sciences, St  
George's University of London, London, UK

<sup>1</sup> Mass Spectrometry Core Laboratory, Edinburgh Clinical Research Facility, Queen's  
Medical Research Institute, University of Edinburgh, Edinburgh, EH16 4TJ

<sup>2</sup> BHF Centre for Cardiovascular Science, Queen's Medical Research Institute, University of  
Edinburgh, Edinburgh, EH16 4TJ

<sup>3</sup> Dept of Neuroscience, Reproductive Sciences and Dentistry, University of Naples  
Federico II, Naples, Italy.

This article has been accepted for publication and undergone full peer review but has not been  
through the copyediting, typesetting, pagination and proofreading process which may lead to  
differences between this version and the Version of Record. Please cite this article as doi:  
10.1111/bph.15947

<sup>4</sup> Department of Molecular Physiology and Biophysics, Robert M. Berne Cardiovascular Research Centre, University of Virginia School of Medicine, Virginia, United States.

Word count: 3999

Corresponding Author:

- Name: Iain A Greenwood
- Address: Vascular Biology Research Centre, Institute of Molecular and Clinical Sciences, St George's University of London, London, UK
- Email: [grenwood@sgul.ac.uk](mailto:grenwood@sgul.ac.uk)
- Phone number: 020 8672 9944- 2857

Acknowledgements

The authors would like to thank Miss Hericka B Figueriedo for her contribution to the pilot data which formed the basis for this study and the image resource facility at St George's university, London. SNB was funded by the British Heart Foundation (Grant #FS/18/41/33762) awarded to IAG. For work conducted in the University of Edinburgh Clinical Research Mass Spectrometry Core Facility (RRID:SCR\_021833) we are grateful to Scott Denham, Jo Simpson and Tricia Lee for their technical expertise.

Conflict of interest

The authors declare no conflict of interest.

## Nomenclature of Targets and Ligands

Key protein targets and ligands in this article are hyperlinked to corresponding entries in <http://www.guidetopharmacology.org>, and are permanently archived in the Concise Guide to PHARMACOLOGY 2021/22 (Alexander *et al.*, 2021).

## Declaration of transparency and scientific rigour

This Declaration acknowledges that this paper adheres to the principles for transparent reporting and scientific rigour of preclinical research as stated in the BJP guidelines for Natural Products Research, Design and Analysis, Immunoblotting and Immunochemistry, and Animal Experimentation, and as recommended by funding agencies, publishers and other organisations engaged with supporting research.

## Data availability

The data generated herein is available upon reasonable request to the corresponding author.

## Ethics approval statement

Animals used within the following investigation were handled in strict accordance with the Animal (Scientific Procedures) Act 1986.

## Author contribution statement

SNB and EAF performed the functional and molecular research. NZMH and RA executed and interpreted the steroid assays. BEI provided essential tools and reagents. SNB and IAG wrote the manuscript. SNB, VB, JBS and IAG designed the

research study. All authors contributed to the manuscript and approved the submitted version.

## Abstract

*Background and purpose:* *Kcnq*-encoded Kv7 channels (termed Kv7.1-5) regulate vascular smooth muscle cell (VSMC) contractility at rest and as downstream targets of receptor mediated responses. However, the current literature focuses predominantly on males. Considering the known impact of sex, the oestrus cycle and sex-hormones on vascular reactivity, the aim of this investigation was to characterise the molecular and functional properties of Kv7 within renal and mesenteric arteries from female Wistar rats separated into Di-oestrus and Met-oestrus (F-D/M) and Pro-oestrus and Oestrus (F-P/E).

*Experimental approach:* RT-qPCR, immunocytochemistry, proximity-ligation assay and wire myography were performed in renal and mesenteric arteries. Circulating sex-hormone concentrations was determined by liquid chromatography tandem mass-spectrometry. Whole-cell electrophysiology undertaken on cells expressing Kv7.4 in association with G-protein coupled Oestrogen receptor 1 (GPER1).

*Key results:* The Kv7.2-5 activators S-1/ML213 and the pan-Kv7 inhibitor Linopirdine were more effective in arteries from F-D/M compared to F-P/E animals. In VSMCs isolated from F-P/E rats, the membrane abundance of Kv7.4 but not Kv7.1, Kv7.5 and Kcne4 was reduced compared to F-D/M cells. Plasma oestradiol was significantly higher in F-P/E compared to F-D/M and progesterone showed the converse pattern. Oestradiol/GPER1 agonist G-1 diminished Kv7.4 currents in heterologous expression system and reduced Kv7.4 membrane abundance, ML213 relaxations, and interaction

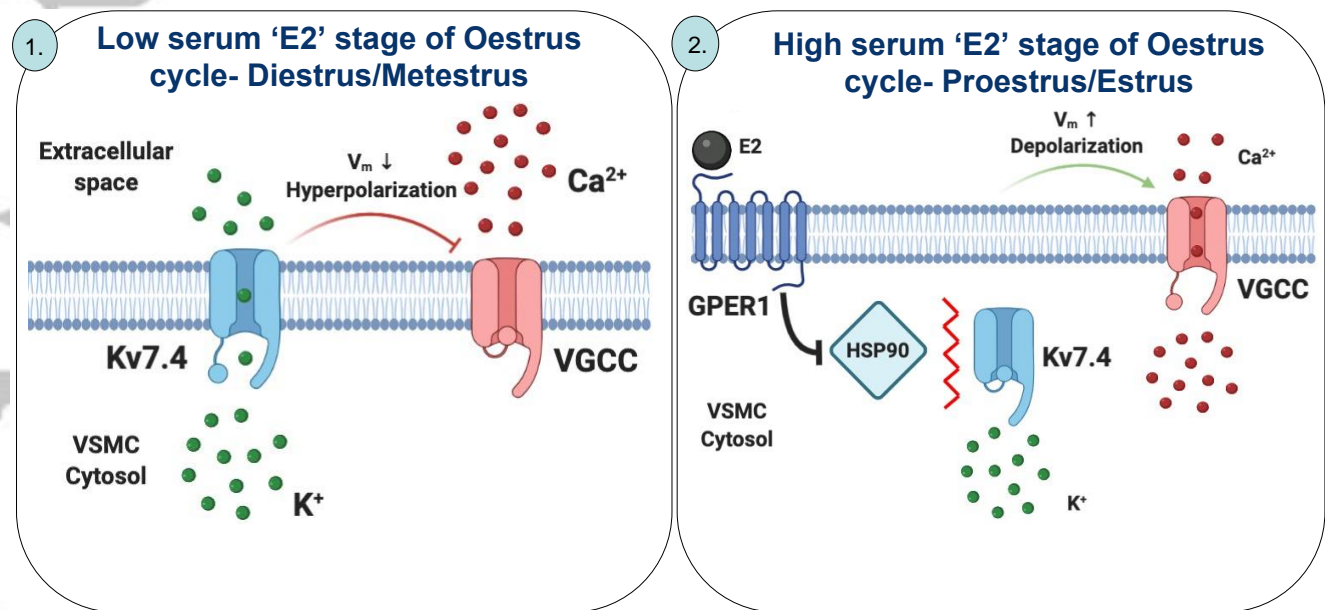
between Kv7.4 and the molecular chaperone protein, heat shock protein 90 (HSP90), in arteries from F-D/M but not F-P/E.

*Conclusions and implications:* GPER1 signalling decreases Kv7.4 membrane abundance in conjunction with diminished interaction with HSP90, giving rise to a 'pro-contractile state.'

#### Abbreviations

- $\alpha$ -smooth muscle cell actin (*Acta-2*)
- Large conductive calcium activated potassium channel (BK<sub>Ca</sub>)
- Platelet endothelial cell marker 1 (*Cd31*)
- Oestradiol (E2)
- Endothelium denuded (EC(-))
- Endothelium intact (EC(+))
- Endothelial cells (ECs)
- Di-oestrus and Met-oestrus (F-D/M)
- Follicular stimulating hormone (FSH)
- Pro-oestrus and Oestrus (F-P/E)
- G-protein coupled oestrogen receptor 1 (GPER1)
- Heat shock protein 90 (HSP90)
- HEK-Kv7.4 cells transiently transfected with *GPER1* (HEK-Kv7.4-GPER1)
- Human embryonic kidney 293B stably expressing Kv7.4 (HEK-Kv7.4)
- High K<sup>+</sup> physiological salt solution (K<sup>+</sup>PSS)
- Voltage-gated potassium channel (Kv)
- ATP-sensitive potassium channel (K<sub>ATP</sub>)

- Targeted liquid chromatography-tandem mass spectrometry (LC-MS/MS)
- Luteinizing hormone (LH)
- Proximity ligation assay (PLA)
- Physiological salt solution (PSS)
- Voltage-gated calcium channels (VGCC)
- Vascular smooth muscle cells (VSMCs)



What is already known

- Vascular Kv7 channels are key components of resting tone and endogenous vasoactive responses.
- The Oestrus cycle regulates vascular reactivity.

What this study adds

- Oestrus cycle dependent reduction in Kv7.4 membrane abundance and function coincided with a pro-contractile phenotype.
- GPER1 activation negatively regulates Kv7.4 forward trafficking and function.

Clinical significance

- Oestrogenic signalling decreases vascular Kv7 channel function.
- Negative regulation of Kv7.4 may contribute the detrimental attributes of hormone replacement therapy.

Accepted Article

## 1 Introduction

Sexual dimorphisms in cardiovascular physiology and pathophysiology are a well-documented phenomenon (Pabbidi *et al.*, 2018). Pre-menopausal women exhibit greater coronary and cerebral blood flow and the incidence of adverse cardiovascular events is significantly lower (Pabbidi *et al.*, 2018). As the female cardioprotective phenotype diminishes post-menopause, the most likely candidates that drive sexual dimorphisms within the vasculature are sex-hormones, primarily oestrogens. However, the role of oestrogens within the cardiovascular system remains enigmatic, being shown to be both protective and detrimental to the vasculature (Hulley *et al.*, 1998, 2002; Yang & Reckelhoff, 2011).

Within rodent and human arteries, *KCNQ*-encoded Kv7 channels are key regulators of vascular reactivity, whereby activation of the channel mediates hyperpolarisation of the membrane and closure of voltage gated calcium channels (VGCC). Of the five subtypes; *KCNQ1*, *KCNQ4* and *KCNQ5* are the principally expressed transcripts in vascular smooth muscle (Ng *et al.*, 2011; Ohya *et al.*, 2003), Kv7.4 is the predominantly expressed protein (Ng *et al.*, 2011; Yeung *et al.*, 2007) and the Kv7.4/Kv7.5 heterotetramer is purported to be the most common channel species (Chadha *et al.*, 2014). Pharmacological and molecular evidence demonstrates that Kv7.4/Kv7.5 activity regulates resting membrane potential (Mackie *et al.*, 2008) and is functionally important for cAMP- and cGMP-linked receptor mediated vasorelaxation (Chadha *et al.*, 2012, 2014; Stott *et al.*, 2015; Mondéjar-Parreño *et al.*, 2019) and PKC-mediated contraction (Brueggemann *et al.*, 2006). Notably, Kv7.4 channels are downregulated in hypertensive rats (Jepps *et al.*, 2011) via post-transcriptional mechanisms affecting protein synthesis, trafficking and degradation (Carr *et al.*, 2016;



Barrese *et al.*, 2018) and are associated with the hypertensive phenotype (Barrese, Stott & Greenwood, 2018).

To date, literature on vascular Kv7 channels focuses primarily on arteries from male animals. Considering known sexual dimorphisms in vascular reactivity and the growing appreciation for sex as an experimental factor (Docherty *et al.*, 2019), we aimed to address this deficit. We characterised Kv7 channel functional and molecular properties within arteries from female Wistar rats. In light of previously demonstrated oestrus cycle dependent changes in vascular reactivity (Jaimes *et al.*, 2019), the oestrus cycle was a key consideration in the following study. The rat oestrus cycle lasts only 4-5 days, with each stage lasting the following: 1.) Pro-oestrus-14 hrs; 2.) Oestrus-24-48 hrs; 3.) Met-oestrus-6-8 hrs; 4.) Di-oestrus-48-72 hrs (Cora, Kooistra & Travlos, 2015). As sex-hormones peak in Pro-oestrus (Nilsson *et al.*, 2015), females were separated into Pro-oestrus and Oestrus (F-P/E), and Di-oestrus and Met-oestrus (F-D/M) stages of the oestrus cycle. The observations detailed herein demonstrate a remarkable oestrus cycle-derived reduction in Kv7.4 membrane abundance by oestradiol (E2) signalling via G-protein coupled oestrogen receptor-1 (GPER1), which underpins a pro-contractile vascular state.

## 2 Methods and materials

### 2.1 Animal model

Experiments were performed on male and female Wistar rats (RRID:RGD\_734476; Charles River, Margate, UK) ages 11-15 weeks (200-350g) kept at the Biological Research Facility (St George's University, London). The animals were housed in cages with free access to water and food (RM1; Dietex International, UK) on a 12-

hour light/dark cycle and maintained at a constant temperature and humidity ( $21^{\circ}\text{C} \pm 1^{\circ}\text{C}$ ;  $50\% \pm 10\%$  humidity) in accordance with the Animal (Scientific Procedures) Act (ASPA) 1986. Animals were kept in a bedding of LSB Aspen woodchip. Female rats were housed separately from males to ensure standard progression through the oestrus cycle. Animals were culled by cervical dislocation with secondary confirmation via femoral artery severance in accordance with Schedule 1 of the ASPA 1986. Organs were harvested and immediately placed in ice cold physiological salt solution (PSS), composition ( $\text{mmol}\cdot\text{L}^{-1}$ ): 119 NaCl, 4.5 KCl, 1.17  $\text{MgSO}_4\cdot 7\text{H}_2\text{O}$ , 1.18  $\text{NaH}_2\text{PO}_4$ , 25  $\text{NaHCO}_3$ , 5 glucose, 1.25  $\text{CaCl}_2$ . 2 mL of blood was harvested following euthanasia into vials containing 100 $\mu\text{L}$  of the anti-coagulant Ethylenediaminetetraacetic acid. Samples were subsequently centrifuged at 2000 rcf for 20 minutes. Serum was extracted and stored at  $-80^{\circ}\text{C}$ .

## 2.2 Oestrus cycle stage determination

Following euthanasia, 50 $\mu\text{L}$  of PSS was inserted into the vaginal canal via a 2-200 $\mu\text{L}$  tip and flushed 4-6 times to liberate cells from the surface of the cervix. PSS was removed from the vaginal canal and 25 $\mu\text{L}$  of the subsequent cell suspension was mounted on a glass slide and examined under light microscopy. Variation in the population of three principal cell types were used to identify each stage, including; large keratinised (cornified) epithelial cells, nucleated epithelial cells and leukocyte as previously described by (Cora, Kooistra & Travlos, 2015) which was the primary tool used for cycle stage determination during the course of this study. Representative images of each cycle stage are shown in Figure S1. To generate the representative images in Figure S1, 50 $\mu\text{L}$  of cervical cell suspension was plated on a glass slide and

left to adhere for 1 hr at RT. Subsequently, 1 mL of Toluidine blue (made in house), was passed through a 0.2 $\mu$ M syringe filter flooding the slide. Cells were left in dye for 45 seconds, before being submerged in distilled water on a rotating plate (20rpm) for 1min. Cells were left to dry, then imaged via Nikon Eclipse Ni. Cycle stage determination was performed post-experiment during functional investigation as a means of blinding, this was not possible during molecular techniques.

### 2.3 Wire Myography

Arterial segments (~2mm) of main renal, 2<sup>nd</sup> order mesenteric, basilar and left anterior descending coronary arteries were mounted on either 200 $\mu$ m pins (renal) or 40 $\mu$ m tungsten wire (mesenteric, coronary and cerebral arteries) within a myograph chamber (Danish Myo Technology, Arhus, Denmark) containing 5mL of PSS oxygenated with 95% O<sub>2</sub> and 5% CO<sub>2</sub> at 37°C. Vessels then underwent a passive force normalisation process to achieve an internal luminal circumference at a transmural pressure of 100 mmHg (13.3 kPa) to standardise pre-experimental conditions (Mulvany & Halpern, 1976). Force generated was amplified by a PowerLab (ADInstruments, Oxford, UK), then recorded via LabChart software (RRID:SCR\_017551; ADInstruments, Oxford, UK). Vessels were then left to rest for 10 minutes. A minimal interval that was applied between all separate challenges to the vessels. Isotonic high K<sup>+</sup> physiological salt solution (K<sup>+</sup>PSS) of the following composition (mmol-L<sup>-1</sup>); 63.5 NaCl, 60 KCl, 1.17 MgSO<sub>4</sub>·7H<sub>2</sub>O, 1.18 NaH<sub>2</sub>PO<sub>4</sub>, 25 NaHCO<sub>3</sub>, 5 glucose, 1.25 CaCl<sub>2</sub> was then added to bath to determine vessel viability. After the contraction had stabilised, the vessels were washed in normal PSS until they returned to baseline. Vessels were then challenged again with K<sup>+</sup>PSS to ensure maximal contraction had been achieved. Endothelial cell (EC) integrity was determined by relaxation of pre-constricted arterial tone (10 $\mu$ mol-L<sup>-1</sup>

<sup>1</sup>  $\alpha$ 1-adrenoceptor agonist Methoxamine) in response to  $10\mu\text{mol-L}^{-1}$  synthetic acetylcholine analogue Carbachol. Only vessels that generated  $\geq 80\%$  relaxation were used and considered endothelium positive. When generating concentration effect curves in response to thromboxane A2 receptor agonist U46619 ( $0.003\text{-}3\mu\text{mol-L}^{-1}$ ), logarithmically increasing concentrations of an agent were added to the bath following the 'warm-up' protocol, with incremental increase in tension allowed to plateau before the next concentration was added. Upon completion of the curve, vessels were washed in standard PSS and allowed to return to base-line tension. Vessels were then pre-incubated in either DMSO solvent control, Linopirdine ( $10\mu\text{mol-L}^{-1}$ ) or HMR-1556 ( $10\mu\text{mol-L}^{-1}$ ) for 10mins prior to starting a second concentration effect curve. All contractions were then normalised to the peak, stable contraction generated in response to  $\text{K}^+\text{PSS}$ . In contrast, when investigating vasorelaxants, vessels were first pre-constricted with  $300\text{nmol-L}^{-1}$  TXA2 receptor agonist U46619. Once tone had stabilised logarithmically increasing concentrations of either Isoprenaline ( $0.003\text{-}3\mu\text{mol-L}^{-1}$ ), S-1 ( $0.1\text{-}10\mu\text{mol-L}^{-1}$ ), ML213 ( $0.01/0.1\text{-}10\mu\text{mol-L}^{-1}$ ), NS11021 ( $0.1\text{-}30\mu\text{mol-L}^{-1}$ ), Pinacidil ( $0.1\text{-}30\mu\text{mol-L}^{-1}$ ) or Nicardipine ( $0.001\text{-}1\mu\text{mol-L}^{-1}$ ) were then added to the bath. With regards to Isoprenaline, vessels were then washed, pre-incubated in either DMSO solvent control, Linopirdine ( $10\mu\text{mol-L}^{-1}$ ) or HMR-1556 ( $10\mu\text{mol-L}^{-1}$ ) for 10mins, and a second curve was generated. With experiments involving vasorelaxation in response to ion channel modulators, only one curve could be generated as these drugs do not readily wash out. EC denudation was achieved by mechanical abrasion of lumen with human hair and was validated by an ablation of the relaxation of pre-contracted arterial tone ( $10\mu\text{mol-L}^{-1}$  methoxamine) in response to carbachol.

## 2.4 Reverse transcription quantitative polymerase chain reaction

Relative fold-changes in expression levels of *Kcnq1-5*, *Kcne1-5*, hormone receptor and EC/vascular smooth muscle cell (VSMC) marker transcript were determined in main renal and mesenteric arteries and whole brain, heart, and uterine samples via Reverse transcription quantitative polymerase chain reaction (RT-qPCR). In addition, endothelium intact (EC(+)) and endothelium denuded (EC(-)) lysates of mesenteric arteries were prepared. EC(-) samples were prepared as previously (Askew Page *et al.*, 2019).

mRNA was extracted and converted to cDNA using Monarch Total RNA Miniprep Kit (New England BioLabs, Ipswich, Massachusetts, USA) then LunaScript RT SuperMix Kit (New England BioLabs, Ipswich, Massachusetts, USA) respectively. Quantitative analysis of target genes was assessed via CFX-96 Real-Time PCR Detection System (RRID:SCR\_018064; BioRad, Hertfordshire, UK). Samples were run in BrightWhite qPCR plates (Primer Design, Camberley, UK) in combination with PrecisionPLUS qPCR Master Mix (Primer Design, Camberley, UK), 300nmol-L<sup>-1</sup> of gene specific target primer (ThermoFisher scientific, Waltham, Massachusetts, USA) and 10ng cDNA as per manufacturers instruction. Quantification cycle (Cq) was determined via Bio-Rad CFX96 Manager 3.0. Cq were normalised to the average of two housekeeping genes chosen among ubiquitin C (*Ubc*), polyamine transporter 1 (*Tpo-1*), cytochrome C1 (*Cyc1*), Calnexin (*Canx*), and glyceraldehyde 3-phosphate dehydrogenase (*Gapdh*), and expressed using either formula  $2^{-\Delta Cq}$  or  $2^{-\Delta\Delta Cq}$  for analysis of relative abundance or relative fold changes as stated (Jepps *et al.*, 2011). See table 1 for a list of the primers used in the following investigation (ThermoFisher, Paisley,

UK). Primers for house keepers were provided by Primer design (UK), as such sequences cannot be disclosed for proprietary reasons.

## 2.5 Vascular smooth muscle cell isolation

Renal and mesenteric arteries were incubated in isolation PSS of the following composition ( $\text{mmol-L}^{-1}$ ): 120 NaCl, 6 KCl, 12 glucose, 10 HEPEs and 1.2  $\text{MgCl}_2$  supplemented with 1.75mg/mL Collagenase Type IA, 0.9mg/mL protease, 1mg/mL Trypsin inhibitor and 1mg/mL bovine serum albumin (Sigma, UK) at 37°C for 30 min (renal artery) and 17 min (mesenteric artery). Next, vessels were gently triturated with wide-bore glass pipette to liberate VSMCs from their extracellular matrix. The subsequent cell suspension was supplemented with 2.5  $\text{mmol-L}^{-1}$   $\text{Ca}^{2+}$  and left to adhere on 25mm glass coverslips for 1hr in an incubator at 37°C in 95%  $\text{O}_2$  + 5%  $\text{CO}_2$ . Isolated myocytes were then either fixed immediately afterwards or were incubated in 1mL isolation PSS containing DMSO + Ethanol, E2 (10 $\text{nmol-L}^{-1}$ ), E2 + G36 (1 $\mu\text{mol-L}^{-1}$ ) or G-1 (1 $\mu\text{mol-L}^{-1}$ ) for 10 min or 30 min as stated.

## 2.6 Immunocytochemistry

Isolated VSMCs were fixed in 3% PFA containing phosphate buffered serum (PBS) for 15 min at room temperature (Barrese *et al.*, 2018). For membrane staining cells were incubated in Alexa Fluor 488-conjugated wheat germ agglutinin (WGA; Thermo-Fisher, Paisley, UK; dil. 1:200 in PBS) for 10mins, washed in 0.1  $\text{mmol-L}^{-1}$  glycine in PBS for 5 min and incubated in blocking solution (0.1% Triton X-100, 10% foetal bovine serum in PBS) for 1 hr. Cells were incubated overnight in either Rabbit Anti-Kv7.4 (RRID:AB\_2341042; #APC-164; Alomone, Jerusalem, Israel; dil. 1:200), Rabbit Anti-Kv7.1 (Pineda, Antikörber-Service, Germany; dil. 1:100), Rabbit Anti-Kv7.5

(RRID:AB\_210806; #ABN1372; Millipore, Temecula, CA, USA; dil. 1:100) or Rabbit Anti-Kcne4 (RRID:AB\_1079170; #HPA011420; Atlas Antibodies, Sweden; dil. 1:200) at 4°C. Cells were then washed in PBS and incubated in goat anti-rabbit secondary anti-body conjugated to Alexa Fluoro 568 (RRID:AB\_143157; A11036; Thermo-Fisher, Paisley, UK; dil. 1:100), then mounted in Vectasheild (P4170; Sigma, UK) medium containing 4',6-diamidino-2-phenylindole (DAPI). All anti-bodies were diluted in blocking solution. Cells were then imaged via Nikon A1R confocal microscope (inverted) on Ti2 chassis (Image Resource Facility, St George's University, London). For experiments determining Membrane:Cytosol ratio for Kv7.4 expression, fluorescence intensity profiles for Kv7.4 and WGA were plotted across three randomly drawn lines spanning the width of the cell measured in arbitrary units (A.U.) using image J software (RRID:SCR\_003070; <https://imagej.nih.gov/ij/>). Fluorescence intensity  $\geq 200$  A.U was considered as the plasma membrane and below the threshold was considered as the cytosol. Membrane:Cytosol ratio for Kv7.4 expression was calculated by measuring the average fluorescence intensity of Kv7.4 within the membrane and dividing it by the average fluorescence intensity of Kv7.4 within cytosol. 10-12 cells per *n*. Total cell fluorescence was measured by via Image J software (<https://imagej.nih.gov/ij/>). Validation of Rabbit Anti-Kv7.4 (#APC-164) is demonstrated in supplemental figure 2 (Fig S2).

## 2.7 Serum concentration of sex hormones

Steroid analysis was performed by targeted liquid chromatography-tandem mass spectrometry (LC-MS/MS), following extraction of samples through automated supported liquid extraction (SLE) on an Extrahera liquid handling robot (Biotage, Uppsala, Sweden) adapted from Boulton *et al* (2021). The method has an intra- and

inter assay coefficient variation between 4.9-7.2% for the five steroids measured; E2, aldosterone, testosterone, androstenedione and progesterone. Analysis was performed on an I-class Acquity UPLC (Waters, Wilmslow, UK) interfaced to a QTRAP 6500+ (AB Sciex, Warrington, UK) mass spectrometer. Instrument control and data acquisition were achieved using Analyst® 1.6.3 Software. Data were integrated and evaluated using MultiQuant® 2.3.1 (AB Sciex, Warrington, UK). Chromatographic separation was achieved on a Kinetex C18 (2.1 x 150 mm; 2.6 µm particle size), column fitted with a KrudKatcher Ultra In-Line Filter (0.5 µm porosity) both from Phenomenex, UK. The mobile phase system was water and methanol with ammonium fluoride (50 µM) as modifier at a flow rate of 0.3 mL/min over 16 minutes, starting at 55% B for 2 mins, rising to 100% B over 6 minutes, held for 2 mins, before returning to 55% B over 0.1 mins and equilibrating for 4.9 minutes, all held at a temperature of 50°C. The solvent flow was diverted to waste from 0-2 mins and 11 -16 mins. The mass spectrometer was operated in electrospray ionisation mode with polarity switching using a TurbolonSpray source and data were collected in unit resolution (0.7 *m/z* full width at half maximum). The source was operated at 600°C with polarity switching with an IonSpray voltage of 5.5 kV/-4.5 kV, a curtain gas of 30 psi, nitrogen nebuliser ion source gas 1 and heater ion source gas 2 of 40 psi and 60 psi, respectively. Multiple reaction monitoring transitions for steroids and their isotopically labelled internal standards are as follows with chromatographic retention time; Negative ions following -4.5 kV ionspray voltage for 17β-oestradiol (7.0 mins) *m/z* 271.0 → 144.9, 182.9 at -21V and -19V, <sup>13</sup>C<sub>3</sub>-[2,3,4]-oestradiol (7.0 mins) *m/z* 274.0 → 147.9 at -29V, aldosterone (2.6 mins) *m/z* 359.1 → 188.9, 331.0 at -21 and -35V and d8-aldosterone (2.6 mins) *m/z* 367.2 → 193.9 at -21V. Positive ions for testosterone (7.6 mins) *m/z* 289.1 → 97.0, 109.2 at 12V and 6 V, <sup>13</sup>C<sub>3</sub>-[2,3,4]-



testosterone (7.6 mins)  $m/z$  292.1  $\rightarrow$  100.0 at -12V, androstenedione (6.8 mins)  $m/z$  287.1  $\rightarrow$  97.0, 78.9 at 14 and 10 V,  $^{13}\text{C}_3$ -[2,3,4]-androstenedione (6.8 mins)  $m/z$  290.2  $\rightarrow$  100.1 at -14V and progesterone (8.9 mins)  $m/z$  315.0  $\rightarrow$  97.1, 109.1 at 25 and 27 V and 2,2,4,6,6,17 $\alpha$ ,21,21,21-d9-progesterone (8.9 mins)  $m/z$  324.1  $\rightarrow$  100.0, 109.1 at 15 V.

Calibration ranges (between 0.0025 – 100 ng/mL) for each steroid were plotted as the peak area ratio of the analyte divided by the relevant internal standard versus amount of steroid. Amounts of steroid were calculated using the calibration lines of best fit, which were considered acceptable if the regression coefficient,  $r$ , was  $>0.99$ , with  $1/x$  weighting.

Serum concentration of Luteinizing hormone (LH) and follicular stimulating hormone (FSH) were determined at the University of Virginia Ligand Core for clinical and basic scientific research. Hormones were analysed via an own in-house enzyme-linked immunoblot assay (ELISA) protocol. LH was measured in serum by a two-step sandwich immunoassay using monoclonal antibodies against bovine LH (no. 581B7) and against the human LH-beta subunit (no. 5303: Medix Kauniainen, Finland) as described previous (Haavisto *et al.*, 1993). FSH was assayed by RIA using mouse FSH reference prep AFP5308D for assay standards and Mouse FSH antiserum (guinea pig; AFP-1760191). See (<https://med.virginia.edu/research-in-reproduction/ligand-assay-analysis-core/>) for further detail.

## 2.9 Single cell electrophysiology

Human embryonic kidney 293B (HEK293B) cells stably expressing human Kv7.4 (HEK-Kv7.4; Copenhagen, Denmark), were grown in DMEM/F-12 (Sigma, UK) supplemented in 1% penicillin / streptomycin in 5% CO<sub>2</sub> at 37°C. HEK-Kv7.4 cells were transiently transfected with *GPER1* (HEK-Kv7.4-GPER1; HG11264-ACG; pCMV3-GPER1-GFPspark; 4µg; Sino Biological, Eschborn, Germany) via Lipofectamine 3000 reagent (ThermoFisher scientific, Waltham, Massachusetts, USA) as per manufacturer's instructions. HEK-Kv7.4-GPER1 and same day non-transfected controls were mounted on glass coverslips and left to attach for 1hr at room temperature. Cells were then incubated in either solvent, E2 (10nmol-L<sup>-1</sup>) or G-1 (1µmol-L<sup>-1</sup>) for 30 min prior to generating ruptured whole-cell current recordings.

Coverslips were mounted on an inverted microscope fitted with a Nikon C-SHG mercury lamp. Cells were bathed in an external solution composed of (in mmol-L<sup>-1</sup>): 140 NaCl, 4 KCl, 2 CaCl<sub>2</sub>, 10 HEPES, 1 MgCl<sub>2</sub> balanced to a pH of 7.4 with NaOH at room temperature. Glass pipettes (Plowden & Thompson) were pulled in house via PP-830 (Narishige, Japan) to a resistance of 6-10 MΩ. Pipettes were filled with an internal solution composed of (in mmol-L<sup>-1</sup>): 110 K gluconate, 30 KCl, 0.5 MgCl, 5 HEPES, 0.5 EGTA, 1 Na<sub>2</sub>ATP. All currents in the following investigation were recorded using an AXOpatch 200B amplifier (Axon instruments) and Whole cell-electrical signals were made and digitized via Digidata 1550A series operated by pClamp 10.7 (Molecular Devices). After membrane rupture cells were held at -50 mV and pulsed to +20 mV every 20 sec for 200 ms. Once currents had stabilised current voltage relationships (*I/V*) were constructed by stepping from -50 mV to 'test voltages' ranging from -70 mV to +40 mV for 1.5 sec. Peak current amplitude normalised to cell size,

$I_{(pA/pF)}$  was measured following plateau at each voltage-step. Voltage was stepped down to an inactivation step of +40 mV after each test and measured as a 'tail current.'

## 2.9 Proximity ligation assay

The interaction of Kv7.4 and heat shock protein 90 (HSP90) was determined by proximity ligation assay (PLA) similar to Barrese *et al* (2018). Mesenteric VSMCs were isolated, incubated in either ethanol or  $10\text{nmol-L}^{-1}$  E2 and fixed as above. Cells were washed in  $0.1\text{ mmol-L}^{-1}$  glycine containing PSS for 10mins, permeabilised via 0.1% triton X-100 for 5mins and blocked via Duolink blocking solution for 1 hr at  $37^{\circ}\text{C}$ , then incubated overnight in a combination of rabbit anti-Kv7.4 (APC-164, Alamone, Jerusalem, Israel; dil 1:200) and mouse-anti-HSP90 (RRID:AB\_300396; ab13492, Abcam, Cambridge, UK; dil 1:200) overnight at  $4^{\circ}\text{C}$ . Cells were incubated in a combination of Duolink In situ PLA probes, anti-mouse MINUS (RRID:AB\_2713942; DUO92004; Sigma-Aldrich, St Louis, MO, USA) and anti-rabbit PLUS (RRID:AB\_2810940; DUO92002; Sigma-Aldrich, St Louis, MO, USA) for 1hr at  $37^{\circ}\text{C}$ , as per manufacturer's instructions. Using Duolink In situ detections reagents (DUO92008; Sigma-Aldrich, St Louis, MO, USA) samples underwent ligation (30 min at  $37^{\circ}\text{C}$ ) and amplification (100 min at  $37^{\circ}\text{C}$ ) as per manufacturer's instructions. Cells were then mounted on cover slides in Vectasheild (P4170; Sigma, UK) containing DAPI. All anti-bodies and probes were diluted in blocking solution. Cells were then imaged in the Image Resource Facility, St George's University, London.

## 2.10 Data analysis

All functional figures show mean data from at least 5 animals  $\pm$  standard error of the mean (SEM). For quantitative analysis of immunocytochemistry, at least 10 cells were

gathered per biological repeat. For functional experiments involving cumulative concentrations, a transformed data set was generated using;  $X = \text{Log}(X)$ , to reduce representative skew. Following which a four parametric linear regression analysis was performed using the following equation; (Log(Agonist) vs. response – Variable slope (four parameters Bottom/Hillslope/top/ $EC_{50}$ )) using GraphPad Prism (RRID:SCR\_002798; Version 8.2.0) to fit a concentration effect curve to the figure. For data comparing multiple groups, a One way-ANOVA was performed, or Two way-ANOVA followed by a *post hoc* Bonferonni/Dunnet's test, to account for type 1 errors in multiple comparisons was performed for comparison of mean values. Multiple comparisons include condition A vs condition B at varying concentrations. Significance values are represented as follows;  $P \leq 0.05$  (\*/#/\$). Investigations expressing groups of unequal numbers were gathered due to technical failure or an artefact of cycle stage determination post-experiment during functional investigations. The data and statistical analysis comply with the recommendations of the *British Journal of Pharmacology* on experimental design and analysis in pharmacology in accordance with (Curtis *et al.*, 2018).

## 2.11 Reagents

The reagents used in the present study were: Kv7.2-5 specific activators S-1 and ML213 (Jepps *et al.*, 2014; Baldwin *et al.*, 2020); pan-Kv7 blocker Linopirdine ( $10 \mu\text{mol-L}^{-1}$ ; Schnee & Brown, 1998); Kv7.1 specific blocker HMR-1556 (Thomas, Gerlach & Antzelevitch, 2003); large conductance calcium activated calcium channel ( $BK_{Ca}$ ) activator NS11021 ( $0.1-10 \mu\text{mol-L}^{-1}$ ); ATP-sensitive potassium channel ( $K_{ATP}$ ) activator Pinacidil ( $0.1-10 \mu\text{mol-L}^{-1}$ ) VGCC channel inhibitor Nicardipine ( $0.001-1 \mu\text{mol-L}^{-1}$ ); thromboxane receptor agonist U46619 ( $0.003-3 \mu\text{mol-L}^{-1}$ ); mixed  $\beta$ -adrenoceptor

agonist Isoprenaline ( $0.003\text{-}3\mu\text{mol-L}^{-1}$ ); the specific GPER1 agonist G-1 (Dennis *et al.*, 2009); the specific GPER1 antagonist G-36 (Dennis *et al.*, 2011). All drugs for isometric tension recordings were obtained from Tocris Bioscience (Oxford, UK) except for S-1 obtained from NeuroSearch (Ballerup, Denmark). Drugs were dissolved in dimethyl sulphoxide (DMSO) or ethanol (E2), and final vehicle concentrations were always  $\leq 0.1\%$ .

### 3 Results

#### 3.1 Oestrus cycle dependent changes in sensitivity to $\text{K}^+$ channel modulators

The  $\text{Kv}7.2\text{-}5$  activator S-1 ( $0.1\text{-}10\mu\text{mol-L}^{-1}$ ) evoked concentration-dependent relaxation of pre-constricted arterial tone ( $300\text{nmol-L}^{-1}$  U46619) in arteries from both F-D/M and F-P/E (see representative traces in Figure 1.A,B). S-1 was approximately 10-fold more potent in renal arteries from F-D/M ( $\text{EC}_{50} = 0.45 \pm 0.07\mu\text{mol-L}^{-1}$ ) rats when compared to arteries from F-P/E rats ( $\text{EC}_{50} = 4 \pm 0.3\mu\text{mol-L}^{-1}$ ; Fig 1.C;  $n=6\text{-}8$ ;  $P \leq 0.05$ ). The same oestrus-cycle-dependent phenomenon was observed within mesenteric, coronary and cerebral arteries (Fig 1.D-F;  $n=4\text{-}8$ ;  $P \leq 0.05$ ).

The structurally dissimilar  $\text{Kv}7.2\text{-}7.5$  activator, ML213 ( $0.1\text{-}10\mu\text{mol-L}^{-1}$ ) was also significantly more potent within arteries from F-D/M rats when compared to arteries from F-P/E rats (Fig 2.A,B;  $n=6$ ;  $P \leq 0.05$ ). Inhibitors of  $\text{Kv}7$  channels depolarise VSMC membrane potential and produce contraction (Mackie *et al.*, 2008). The pan- $\text{Kv}7$  blocker Linopirdine ( $10\mu\text{mol-L}^{-1}$ ) contracted arteries from F-D/M rats more effectively than arteries from F-P/E rats (Fig 2.C-E). In all groups, no contraction was produced by application of  $10\mu\text{mol-L}^{-1}$   $\text{Kv}7.1$  specific blocker HMR-1556 (Fig 2.C,D), consistent with previous reports (Chadha *et al.*, 2012). These data reveal an oestrus cycle dependent contribution of  $\text{Kv}7.2\text{-}7.5$  channels to arterial reactivity.

In contrast, Pinacidil and Nicardipine-dependent relaxations of pre-contracted renal arteries was independent of oestrus cycle stage (Fig 3.B,C;  $n=5-7$ ) whilst NS11021 was ineffective in any stage (Fig 3.A;  $n=5-6$ ). In mesenteric arteries, NS11021 and Nicardipine relaxed pre-contracted tone independent of oestrus cycle stage (Fig 3.D,F;  $n=5-6$ ). Pinacidil was more potent in mesenteric arteries from F-D/M rats compared to F-P/E (Fig 3.E;  $n=5-6$ ;  $P \leq 0.05$ ). No significant differences were observed in the stable pre-contracted tone in response to  $300 \text{ nmol-L}^{-1}$  U46619 ( $\Delta \text{mN}$ ; Fig S3) in either mesenteric or renal arteries harvested from F-P/E or F-D/M Wistars.

### 3.2 Diminished Kv7 channel contribution to receptor mediated responses underpins Oestrus cycle dependent changes in contractility

Kv7 blockers like Linopirdine enhance receptor-mediated contractions (Brueggemann *et al.*, 2006) and diminish cAMP-PKA dependent  $\beta$ -adrenoreceptor mediated vasorelaxation (Chadha *et al.*, 2012, Stott *et al.*, 2018). Within this study, contraction mediated by U46619 ( $0.003-3 \mu\text{mol-L}^{-1}$ ) was less potent within renal arteries from F-D/M compared to F-P/E rats (Fig 4.A,B  $P \leq 0.05$ ;  $n=8-10$ ). Linopirdine significantly augmented the sensitivity of U46619-mediated vasoconstriction within vessels from F-D/M, but not F-P/E rats (Fig 4.A,B;  $P \leq 0.05$ ;  $n=5-10$ ). Within arteries from F-D/M rats pre-incubated in Linopirdine, the response to U46619 was equipotent to arteries from F-P/E rats preincubated in both DMSO solvent control and linopirdine (Fig 4.B). In contrast, pre-incubation with Linopirdine had no effect in arteries from F-P/E rats, and HMR-1556 had no effect within any group (Fig 4.A,B).

Isoprenaline was significantly less potent in renal arteries from F-P/E when compared to vessels from F-D/M rats (Fig 4.C,D;  $n=8-11$ ;  $P \leq 0.05$ ). Similar to previous reports

(Chadha *et al.*, 2012), Linopirdine significantly attenuated Isoprenaline mediated vasorelaxation in arteries from F-D/M rats (Fig 4.C,D;  $n=9-11$ ;  $P\leq 0.05$ ) but had a comparably minor effect on Isoprenaline-mediated vasorelaxation in arteries from F-P/E rats (Fig 4.A-D;  $n=8-9$ ;  $P\leq 0.05$ ). The response to Isoprenaline in arteries from F-D/M rats pre-incubated in Linopirdine was equipotent to arteries from F-P/E rats preincubated in either DMSO solvent control or linopirdine (Fig 4.D). Moreover, in all vessel's pre-incubation with HMR-1556 had no effect (Fig 4.D). See Fig S4 for U46619 mediated contraction and Fig S5 for Isoprenaline mediated relaxation within mesenteric, cerebral, and coronary arteries from F-P/E and F-D/M rats. Within these arteries, where Linopirdine sensitivity was observed, significant differences in control conditions between F-D/M and F-P/E rats were also observed.

The aggregated findings indicate that the Kv7.2-5 channel contribution to Isoprenaline and U46619 mediated vascular response was diminished within arteries from F-P/E rats. This phenomenon potentially underpins the observed oestrus cycle dependent increased sensitivity to TXA2 receptor stimulants and decreased sensitivity to  $\beta$ -adrenoreceptor mediated relaxation in arteries from F-P/E when compared to F-D/M rats.

### 3.3 Identification of Kv7 channel transcript and protein expression in female Wistar arteries

The molecular characteristics of the candidates for vascular Kv7 function was subsequently determined. RT-qPCR revealed no significant differences in *Kcnq1-5* nor  $\beta$ -auxiliary subunit *Kcne1-5* relative transcript abundance within renal and mesenteric arteries from both groups ( $2^{-\Delta Cq}$ ; Fig S6.A-D;  $n=5$ ). Positive control samples

(brain and heart) for transcript expression of target genes can also be seen in supplemental figure 5 (Fig S6.E-H).

Immunocytochemistry of VSMCs isolated from renal and mesenteric arteries of F-D/M Wistar rats revealed Kv7.4 associated fluorescence to be predominantly in the periphery, overlapping with the membrane marker WGA. In contrast, Kv7.4 staining was diffuse throughout the cytosol of VSMCs from F-P/E rats (Fig 5.A,B). The Membrane:Cytosol ratio for Kv7.4 changed from  $1.2 \pm 0.19$  and  $1.8 \pm 0.2$  in renal and mesenteric artery myocytes from F-D/M rats respectively to  $0.5 \pm 0.03$  and  $0.8 \pm 0.02$  within cells from F-P/E rats (Fig 5.C;  $n=3$ ;  $P \leq 0.05$ ). However, no reduction in total cell fluorescence (A.U) was observed between the groups (Fig 5.D). No comparable oestrus cycle dependent differences in staining for the other Kv7 subtypes associated with vascular function, Kv7.1 and Kv7.5, nor the  $\beta$ -auxiliary subunit protein Kcne4 were observed in isolated renal artery VSMCs (Fig S7). Therefore, further experiments focused on Kv7.4 alone.

### 3.4 Cyclical increases in serum Oestradiol mediates a reduction in Kv7.4 membrane abundance via GPER1, impairing ML213 mediated relaxation

To identify potential candidates that drive the observed oestrus cycle dependent fluctuation in Kv7.4 membrane abundance and function, sex steroids were extracted from serum from animals' post-euthanasia. Concentrations of circulating steroidal and gonadal hormones were determined via ELISA and LC-MS/MS (Table 2). Serum E2 was significantly higher within serum harvested from F-P/E rats when compared to F-D/M, whereas serum progesterone was converse (Table 2;  $P \leq 0.05$ ;  $n=8$ ). No



differences between F-D/M and F-P/E were observed with regards to the other hormones investigated (Table 2).

The onset of a pro-contractile phenotype in arteries from F-P/E occurs within a narrow time frame in the absence of a change in the relative abundance of *Kcnq/Kcne* transcripts. In addition, E2 mediated internalisation of Kv7.1 occurs via a fast acting, 'non-genomic' signalling cascade (Alzamora *et al.*, 2011; Rapetti-Mauss *et al.*, 2013). We proposed that a rise in serum E2 during Pro-oestrus mediates a reduction in Kv7.4 membrane abundance in a 'non-genomic' process similar to previous reports (Rapetti-Mauss *et al.*, 2013), that does not recover until Met-oestrus. The three principal E2 receptors include ER $\alpha$  and ER $\beta$ , canonically considered nuclear receptors, and a novel membrane bound receptor, GPER1, are encoded for by *Ers1*, *Ers2* and *Gper1* respectively. We ascertained the expression of these receptors in rat arteries using whole uterine lysates as a positive control. Rat mesenteric and renal artery lysates from both groups had an expression profile of *Esr1*>*Gper1*>*Esr2* whilst the expression profile in uterus was *Esr1*>*Esr2*>*Gper1* (Fig S8.A-C).

We then determined whether short term treatment with E2 could mimic the oestrus cycle-dependent changes in Kv7 responses. Renal and mesenteric arteries from female Wistar rats were incubated with E2 for a period of 5 or 30mins. Within mesenteric and renal arteries from F-D/M, 5mins (black, circle) and 30mins (grey, triangle) of E2 pre-incubation respectively significantly impaired ML213-mediated relaxation (Fig S9.A,C;  $P \leq 0.05$ ;  $n=4-5$ ). E2 had no effect in arteries from F-P/E animals (Fig S9.B,D). Additional experiments were undertaken to determine the long-term and potential genomic effects of E2 incubation on ML213 mediated relaxation of pre-

contracted mesenteric arteries. 4 hour incubation with E2, and vessels that were incubated with E2 for 10mins, then washed and left for 4 hours prior to application of ML213 were compared against vessels pre-incubated in solvent control (Fig S9.E,F). In both conditions, E2 attenuated ML213 mediated relaxation in arteries from F-D/M Wistars only (Fig S9.E,F;  $P \leq 0.05$ ;  $n=5-8$ ).

Pre-incubating renal and mesenteric arteries from F-D/M Wistars with the specific GPER1 agonist G-1 ( $1 \mu\text{mol-L}^{-1}$ ) attenuated ML213-mediated relaxations in a fashion analogous to E2 pre-incubation (Fig 6.A,C;  $n=5-12$ ). Again, G-1 pre-incubation had no effect on renal (Fig 6.B;  $n=6-10$ ) nor mesenteric (Fig 6.D;  $n=6-11$ ) arteries from F-P/E rats. The response to ML213 in mesenteric arteries from F-D/M pre-incubated in E2 ( $EC_{50}=1 \pm 0.17 \mu\text{mol-L}^{-1}$ ) or G-1 ( $EC_{50}=0.9 \pm 0.17 \mu\text{mol-L}^{-1}$ ) mirrored the profile for ML213 seen in mesenteric arteries from F-P/E Wistars pre-incubated in solvent controls ( $EC_{50}=0.84 \pm 0.1 \mu\text{mol-L}^{-1}$  Fig 6.C,D). Moreover, pre-incubating mesenteric arteries with the selective GPER1 antagonist G36 ( $1 \mu\text{mol-L}^{-1}$ ; (Dennis *et al.*, 2011)) prior to application of E2 prevented its inhibitory effects on ML213 mediated relaxation (Fig 6.E;  $P \leq 0.05$ ;  $n=6-8$ ). In contrast, G36 had no effect on ML213 mediated relaxation in arteries from F-P/E rats (Fig 6.F;  $n=5-6$ ).

Incubating isolated mesenteric artery VSMCs from F-DM Wistars in either E2 ( $10 \text{nmol-L}^{-1}$ ) for 10mins (Fig 7.A) or 30mins (Fig 7.B) produced a reduction in the overlap of Kv7.4 staining (Fig 7.A; red) with WGA (Fig 7.A; green) when compared to DMSO/Ethanol control. This led to a reduction in the Membrane:Cytosol ratio for Kv7.4 staining (Fig 7.B,  $P=0.055$ ; D,  $P \leq 0.05$ ;  $n=3$ ) that was analogous to the reduction observed when comparing myocytes from F-D/M and F-P/E (Fig 5). Pre-incubating

isolated VSMCs with the specific GPER1 antagonist G36 for 10mins prior to the application for E2 prevented a reduction in Kv7.4 membrane abundance (Fig 7.C), whereas the GPER1 agonist G-1 replicated E2-mediated Kv7.4 translocation (Fig 7.D). Neither E2 nor G1 had any effect on the predominantly cytosolic staining for Kv7.4 in VSMCs from mesenteric arteries from F-P/E Wistars (Fig S10.A-C). In summary, raised serum E2 during P/E correlated with diminished Kv7.4 membrane abundance and function, and can be mimicked in arteries from F-D/M by GPER1 activation.

E2 and G1 incubation also impaired ML213-mediated relaxations in mesenteric arteries from male rats, whereas relaxations to the BK<sub>Ca</sub> activator NS11021 were unaffected by E2-preincubation (Fig S11; *n*=5).

Compared to E2, little is known of the effect of progesterone on Kv7 function. However, as progesterone was significantly raised in the serum from F-D/M rats we ascertained the potential effects of pre-incubating mesenteric arteries from F-P/E and F-D/M rats in progesterone (10nmol-L<sup>-1</sup>) for 5 and 30 min on ML213-mediated responses (Fig S12). No change in ML213-mediated relaxation was observed in any vessels from either group (Fig S12; *n*=5-8). Consequently, progesterone was not considered in the following investigations, but was helpful in confirming cycle stage.

### 3.5 Oestrogenic inhibition of Kv7 activator mediated relaxation is non-endothelium dependent

A series of experiments were performed to ascertain if the modulatory effects of GPER1 activation was endothelial derived. Similar to our previous findings, removing the endothelium significantly attenuated ML213 mediated relaxation in both

mesenteric arteries from F-D/M and F-P/E rats (Fig 8.A,C;  $P \leq 0.05$ ;  $n=6-7$ ). Pre-incubating EC denuded vessels from F-D/M Wistars with E2 ( $10 \text{ nmol-L}^{-1}$ ) additively attenuated ML213-elicited relaxation (Fig 8.A;  $P \leq 0.05$ ;  $n=6$ ). Whereas, E2 pre-incubation had no effect in EC denuded arteries from F-P/E rats (Fig 8.C;  $n=5-6$ ). The relative fold-change in expression of Oestrogen receptor and VSMC and EC marker transcripts were compared between EC(+) and EC(-) vessels. When comparing relative transcript abundance between EC(-) vs EC(+) whole lysates ( $2^{-\Delta\Delta Cq}$ ), a significant reduction in *Cd31* (platelet endothelial cell marker 1) was observed in conjunction with a significant increase in *Acta2* ( $\alpha$ -smooth muscle actin; Fig.8.E;  $P \leq 0.05$ ;  $n=5$ ). A small increase in *Ers1* and *Ers2* transcripts, and minor decrease in *Gper1* transcripts were observed in EC(-) lysates when compared to EC(+) lysates (Fig.8.E), though this failed to reach significance. In summary, though GPER1 expression was moderately higher within the endothelium, the effect of GPER1 signalling on vascular Kv7.4 appears to originate from within the smooth muscle,

### 3.6 GPER1 activation reduced Kv7.4 currents

Ruptured whole cell recording from HEKs expressing Kv7.4 was used as a secondary means of determining the effect of GPER1 activation on Kv7.4 channel activity. Incubation of HEK-Kv7.4 cells with the GPER1 agonist G-1 ( $1 \mu\text{mol-L}^{-1}$ ) or E2 ( $10 \text{ nmol-L}^{-1}$ ) for 30mins produced a considerable reduction in Kv7.4 currents in cells expressing the GPER1 receptor only (Fig 9). GPER1 stimulation by either G-1 or E2 did not affect voltage of half activation ( $V_{1/2}$ ) of Kv7.4 currents (Fig 9.D). Currents recorded under solvent control conditions were identical in un-transfected and GPER1-expressing HEK cells (Fig 9).

3.7 E2 reduces Kv7.4 interaction with forward trafficking molecular chaperone protein heat-shock protein 90 in F-D/M, but not F-P/E VSMCs

Molecular chaperone protein HSP90 is critical in the folding and biogenesis of potassium channels including  $K_{ATP}$  (Yan *et al.*, 2010), Kv11.1 (Ficker, 2003) and Kv7.4 (Gao *et al.*, 2013). Additionally, GPER1 activation increases human myometrial contractility by phosphorylation of heat shock protein 27 (Maiti *et al.*, 2011) and Angiotensin-II (Ang-II) infusion has been shown to decrease the interaction of Kv7.4 and HSP90 diminishing Kv7.4 membrane abundance (Barrese *et al.*, 2018). Therefore, we proposed that the reduction in Membrane:Cytosol ratio observed in response to E2/G-1 was underpinned by a reduction in interaction of Kv7.4 and HSP90 in a process similar to Ang-II infusion. PLA was used to resolve protein-protein interactions  $\leq 40$ nm, which are expressed as red puncta within the cell. 30min pre-incubation with  $10\text{nmol-L}^{-1}$  E2 reduced the interaction between Kv7.4:HSP90 within mesenteric VSMCs from F-D/M Wistars when compared to Ethanol solvent control ( $P < 0.05$ ;  $n = 3$ ; Fig 10). Comparably, no change in Kv7.4:HSP90 interaction was observed in VSMCs from F-P/E Wistars by E2 (Fig 10.B). Additionally, the puncta per cell in VSMCs from F-P/E rats was equivalent to the that observed in VSMCs from F-D/M pre-incubated in E2.

#### 4 Discussion

In this study, we demonstrate stark oestrus cycle dependent changes in vascular reactivity, whereby pro-contractile vessels from F-P/E rats exhibit diminished Kv7.4 channel function and membrane abundance in conjunction with significantly raised serum E2. Moreover, a F-P/E pro-contractile phenotype could be replicated in pro-relaxant F-D/M rats by both E2 and novel GPER1 activator G-1, a phenomenon that was prevented by the GPER1 specific inhibitor G36. In heterologous overexpression

system, both E2 and G-1 diminished human Kv7.4 currents only in cells transfected with *GPER1*, independent of a change in the biophysical properties of the current and consistent with a reduction in channel number. Finally, E2 diminished Kv7.4 interaction with its forward trafficking molecular chaperone protein HSP90 only in rats in a 'low serum E2' stage of the oestrus cycle.

#### 4.1 Cyclical reduction in Kv7.4 membrane abundance correlates with a pro-contractile phenotype

In spite of the known sexual dimorphisms in cardiovascular physiology and pathophysiology (Pabbidi *et al.*, 2018), little is known about Kv7 channel activity in arteries from females. Of the few studies to consider sex as a factor, Kv7 channels within the female are shown to; 1.) be differentially regulated by its  $\beta$ -auxiliary subunit protein Kcne4 (Abbott & Jepps, 2016); 2.) impair norepinephrine induced increases in total peripheral resistance in normotensive and spontaneously hypertensive female rats only (Berg, 2018).

Here we demonstrate that Kv7.2-5 channel activators S-1 and ML213 relaxed pre-contracted arterial tone in a range of arteries and the pan-Kv7 channel inhibitor Linopirdine and not Kv7.1 specific inhibitor HMR-1556 increased basal tone (Mackie *et al.*, 2008; Chadha *et al.*, 2012; Ng *et al.*, 2011), though significantly more potently and efficaciously in arteries from F-D/M. Additionally, Kv7.2-5 channel inhibition enhanced TXA2-mediated contractions and impaired  $\beta$ -adrenoreceptor-driven relaxations, though more effectively in arteries from F-D/M rats. Immunocytochemistry revealed a corona like staining for Kv7.4 in myocytes from F-D/M renal and mesenteric arteries that was absent in myocytes from F-P/E. However, neither total cell

fluorescence nor the relative abundance of the *Kcnq4* transcripts were altered. Thus, our findings indicate a post-transcriptional cyclical reduction in Kv7.4 membrane abundance, which correlates with diminished contribution of Kv7 channels to both basal tone and receptor mediated responses, contributing to a pro-contractile phenotype. No change in transcript nor membrane abundance of the other candidates for vascular Kv7 channel function were observed (Kv7.1, Kv7.5 and KCNE4), reinforcing the previously reported notion that Kv7.4 is the fundamental component of the functional Kv7.4/Kv7.5 heterotetramer (Barrese, Stott & Greenwood, 2018). However, other ion channels may also be modulated as the present study showed significant oestrus cycle dependent differences in relaxations to the K<sub>ATP</sub> activator pinacidil in mesenteric arteries. Future research will focus on this aspect.

#### 4.2 E2 diminishes Kv7.4 membrane abundance through reduced interaction with HSP90 via GPER1 signalling

When screening for candidates that drive the Oestrus cycle dependent differences in vascular Kv7 activity, our data revealed an increase in serum E2 in F-P/E rats. The role for E2 in modulating vascular reactivity is complex. E2 upregulates the bioavailability of nitric oxide and prostaglandin PGI<sub>2</sub> within ECs, and decreases intracellular calcium availability in VSMCs (Novella *et al.*, 2019; Mazzuca *et al.*, 2015). However, there is less consensus within the literature concerning ion channel modulation by E2. E2 is shown to both increase and decrease the activity of ion channels such as BK<sub>Ca</sub>, K<sub>ATP</sub> and Kv (Kow & Pfaff, 2016). With regards to Kv7, E2 rapidly internalises Kv7.1 in female rat distal colic crypt cells in a fast-acting non-genomic signalling cascade (Rapetti-Mauss *et al.*, 2013; O'Mahony *et al.*, 2007). E2 also diminished *I<sub>Ks</sub>* currents in overexpression models and rabbit cardiac myocytes

(Busch *et al.*, 1996; Möller & Netzer, 2006) but increased M-currents (Kv7.2/3) in mouse Neuropeptide-Y neurons (Roepke *et al.*, 2011). Very little is known of the effect of E2 on vascular Kv7 channels. E2 injection into rats post bi-lateral ovariectomy significantly increased mean arterial pressure (Takezawa *et al.*, 1994). Here, short incubation with supplemental E2 significantly reduced the membrane abundance of Kv7.4, the interaction with its forward trafficking molecular chaperone protein HSP90 and the potency ML213 mediated relaxation in arteries from F-D/M rats in an endothelium independent process. No additive inhibition of Kv7 channel membrane abundance, function nor interaction with HSP90 by E2 was observed in F-P/E rats where serum E2 was higher, supporting a role for oestrogenic signalling in driving the observed cyclical dependent shifts in vasoreactivity.

As the onset of a pro-contractile phenotype during the oestrus cycle occurs within a narrow time frame, we postulated that the effects of oestrogenic signalling were also non-genomic. The candidates for fast-acting oestrogenic signalling include membrane associated GPER1 (Filardo *et al.*, 2000) and ER $\alpha$  following palmitoylation at cysteine residue 446 (Simoncini *et al.*, 2000). As above (O'Mahony *et al.*, 2009, 2007), E2 rapidly reduces colonic crypt cell conductance via ER $\alpha$  downregulation of Kv7.1 via fast acting processes which were PKA-PKC $\delta$  dependent. Here, the effects of extraneous E2 on Kv7.4 function and membrane abundance was replicated by GPER1 specific agonist G-1 (Bologa *et al.*, 2006) and prevented by GPER1 antagonist G36 (Dennis *et al.*, 2011) indicating a role for GPER1 over ER $\alpha/\beta$ . This was supported by single cell electrophysiology in a heterologous over expression system, whereby, E2/G-1 regulation of Kv7.4 was dependent on GPER1 expression. GPER1 activation mediated a reduction in total Kv7.4 current independent of a change in the



conductance of the individual channel, further supporting a role for GPER1. However, as long-term (4hr) incubation with E2 also inhibited ML213 mediated relaxation in vessels from F-D/M rats, we cannot rule out a contribution from nuclear Oestrogen receptors. Further, whilst aldosterone cannot bind GPER1 (Cheng *et al.*, 2014), aldosterone mediates GPER1 dependent sensitisation of Ang-II (Batenburg, Jansen & Bogaerdt, 2012) and phenylephrine mediated contraction (Ferreira *et al.*, 2015). Current understanding indicates that aldosterone mediated GPER1 sensitive vascular effects may be derived from cross talk between mineralocorticoid and oestrogen receptors (Barton & Meyer, 2015). Though we observed no differences in serum aldosterone levels between F-D/M and F-P/E females, future studies that aim to characterise GPER1 signalling should consider receptor cross talk.

Our data suggest that GPER1 activation alters the forward trafficking of Kv7.4 through altered interaction with chaperone HSP90. Ang-II also alters HSP90:Kv7.4 association, resulting in channel ubiquitination and proteasomal degradation (Barrese *et al.*, 2018). We do not know whether similar signaling occurs during the oestrus cycle and channel protein is created *de novo* or ultimate degradation is prevented and the existing Kv7.4 can recycle back to the membrane, as shown previously (Rapetti-Mauss *et al.*, 2013). Moreover, we do not know the signals linking GPER1 activation to HSP90 instability. As there is growing appreciation for the importance of ion channel membrane trafficking as the basis for many channelopathies (Curran & Mohler, 2015), the mechanisms linking GPER1 to HSP90 be the focus of future studies.

### 4.3 Perspectives

Diminished Kv7.4 channel function in response to increased serum E2 has considerable implications. Mean arterial pressure is reportedly higher in the luteal phase of the menstrual cycle (Danborno *et al.*, 2018), a phase historically associated with progesterone production from the corpus luteum. However, Stricker *et al.*, (2006) demonstrated that E2 levels within mid-luteal phase were greater than within the early follicular phase. Further, hormone replacement therapy (HRT) has become one of the most controversial topics of women's health of the last three decades. Trends in disease outcomes for patients on combined Estrogen/Progestin in the Heart and Estrogen/progestin replacement study (HERS) I (Hulley *et al.*, 1998) and II (Hulley *et al.*, 2002) were not favourable, whereby adverse cardiovascular events increased. However there is conflict within the literature (Yang & Reckelhoff, 2011), as animal and human studies on HRT prior to the HERS had positive outcomes. Though the effect of E2 on the prevalence of cardiovascular disease in humans remains enigmatic, an extrapolation of the findings detailed herein could implicate diminished Kv7 channel function in the detrimental attributes of exogenous E2 in rodents and humans, as a reduced Kv7 channel membrane abundance is associated with the hypertensive phenotype. Additionally, aldosterone mediates increased vascular resistance and an increase in blood pressure. Interaction between the mineralocorticoid receptor and GPER1, may diminish Kv7 function, contributing aldosterone mediated changes in blood pressure. GPER1 is largely viewed as a promising therapeutic target in the treatment of cardiovascular disease, we would argue that its effects are currently incompletely understood, meriting further investigation.

## 5 References

- Abbott, G.W. & Jepps, T.A. (2016) Kcne4 Deletion Sex-Dependently Alters Vascular Reactivity. *Journal of Vascular Research*. [Online] Available from: doi:10.1159/000449060.
- Alexander, S.P., Kelly, E., Mathie, A., Peters, J.A., et al. (2021) THE CONCISE GUIDE TO PHARMACOLOGY 2021/22: Introduction and Other Protein Targets. *British journal of pharmacology*. [Online] 178 Suppl 1, S1–S26. Available from: doi:10.1111/bph.15537.
- Alzamora, R., O'Mahony, F., Bustos, V., Rapetti-Mauss, R., et al. (2011) Sexual dimorphism and oestrogen regulation of KCNE3 expression modulates the functional properties of KCNQ1 K<sup>+</sup>channels. *Journal of Physiology*. [Online] Available from: doi:10.1113/jphysiol.2011.215772.
- Askew Page, H.R., Dalsgaard, T., Baldwin, S.N., Jepps, T.A., et al. (2019) TMEM16A is implicated in the regulation of coronary flow and is altered in hypertension. *British Journal of Pharmacology*. [Online] Available from: doi:10.1111/bph.14598.
- Baldwin, S.N., Sandow, S.L., Mondéjar-Parreño, G., Stott, J.B., et al. (2020) KV7 Channel Expression and Function Within Rat Mesenteric Endothelial Cells. *Frontiers in Physiology*. [Online] 11 (December), 1–16. Available from: doi:10.3389/fphys.2020.598779.
- Barrese, V., Stott, J.B., Figueiredo, H.B., Aubdool, A.A., et al. (2018) Angiotensin II Promotes K V 7.4 Channels Degradation Through Reduced Interaction With HSP90 (Heat Shock Protein 90) Novelty and Significance. *Hypertension*. [Online] Available from: doi:10.1161/HYPERTENSIONAHA.118.111116.
- Barrese, V., Stott, J.B. & Greenwood, I.A. (2018) KCNQ-Encoded Potassium Channels as Therapeutic Targets. *Annual Review of Pharmacology and*

*Toxicology*. [Online] Available from: doi:10.1146/annurev-pharmtox-010617-052912.

Barton, M. & Meyer, M.R. (2015) Nicolaus Copernicus and the rapid vascular responses to aldosterone. *Trends in Endocrinology & Metabolism*. 26 (8), 396–398.

Batenburg, W.W., Jansen, P.M. & Bogaardt, A.J. van den (2012) Angiotensin II-aldosterone interaction in human coronary microarteries involves GPR30, EGFR, and endothelial NO synthase. *Cardiovascular Research*. 94, 136.

Berg, T. (2018) Kv7(KCNQ)-K<sup>+</sup>-Channels influence total peripheral resistance in female but not male rats, and hamper catecholamine release in hypertensive rats of both sexes. *Frontiers in Physiology*. [Online] Available from: doi:10.3389/fphys.2018.00117.

Bologa, C.G., Revankar, C.M., Young, S.M., Edwards, B.S., et al. (2006) Virtual and biomolecular screening converge on a selective agonist for GPR30. *Nature chemical biology*. [Online] 2 (4), 207–212. Available from: doi:10.1038/nchembio775.

Boulton, K., Wilson, P.W., Bishop, V.R., Perez, J.H., et al. (2021) Parental methyl-enhanced diet and in ovo corticosterone affect first generation Japanese quail (*Coturnix japonica*) development, behaviour and stress response. *Scientific reports*. [Online] 11 (1), 21092. Available from: doi:10.1038/s41598-021-99812-w.

Brueggemann, L.I., Moran, C.J., Barakat, J.A., Yeh, J.Z., et al. (2006) Vasopressin stimulates action potential firing by protein kinase C-dependent inhibition of KCNQ5 in A7r5 rat aortic smooth muscle cells. *AJP: Heart and Circulatory Physiology*. [Online] 292 (3), H1352–H1363. Available from:

doi:10.1152/ajpheart.00065.2006.

Busch, A.E., Suessbrich, H., Waldegger, S., Sailer, E., et al. (1996) Inhibition of IKs in guinea pig cardiac myocytes and guinea pig IsK channels by the chromanol 293B. *Pflügers Archiv - European Journal of Physiology*. [Online] 432 (6), 1094–1096. Available from: doi:10.1007/s004240050240.

Carr, G., Barrese, V., Stott, J.B., Povstyan, O. V., et al. (2016) MicroRNA-153 targeting of KCNQ4 contributes to vascular dysfunction in hypertension. *Cardiovascular Research*. [Online] Available from: doi:10.1093/cvr/cwv177.

Chadha, P.S., Jepps, T.A., Carr, G., Stott, J.B., et al. (2014) Contribution of Kv7.4/Kv7.5 heteromers to intrinsic and calcitonin gene-related peptide-induced cerebral reactivity. *Arteriosclerosis, Thrombosis, and Vascular Biology*. [Online] 34 (4), 887–893. Available from: doi:10.1161/ATVBAHA.114.303405.

Chadha, P.S., Zunke, F., Zhu, H.L., Davis, A.J., et al. (2012) Reduced KCNQ4-encoded voltage-dependent potassium channel activity underlies impaired  $\beta$ -adrenoceptor-mediated relaxation of renal arteries in hypertension. *Hypertension*. [Online] 59 (4), 877–884. Available from: doi:10.1161/HYPERTENSIONAHA.111.187427.

Cheng, S.-B., Dong, J., Pang, Y., LaRocca, J., et al. (2014) Anatomical location and redistribution of G protein-coupled estrogen receptor-1 during the estrus cycle in mouse kidney and specific binding to estrogens but not aldosterone. *Molecular and cellular endocrinology*. 382 (2), 950–959.

Cora, M.C., Kooistra, L. & Travlos, G. (2015) Vaginal Cytology of the Laboratory Rat and Mouse: Review and Criteria for the Staging of the Estrous Cycle Using Stained Vaginal Smears. *Toxicologic Pathology*. [Online] Available from: doi:10.1177/0192623315570339.

- Curran, J. & Mohler, P.J. (2015) Alternative paradigms for ion channelopathies: Disorders of ion channel membrane trafficking and posttranslational modification. *Annual Review of Physiology*. [Online] 77, 505–524. Available from: doi:10.1146/annurev-physiol-021014-071838.
- Curtis, M.J., Alexander, S., Cirino, G., Docherty, J.R., et al. (2018) Experimental design and analysis and their reporting II: updated and simplified guidance for authors and peer reviewers. *British Journal of Pharmacology*. [Online]. Available from: doi:10.1111/bph.14153.
- Danborn, A.M., Nwankwo, M., Kure, J. & Eluwa, C. (2018) Prevalence of Premenstrual Syndrome and Changes in Blood Pressure with Menstrual Cycle Among University Students. *Nigerian journal of physiological sciences: official publication of the Physiological Society of Nigeria*. 33 (2), 117–124.
- Dennis, M.K., Burai, R., Ramesh, C., Petrie, W.K., et al. (2009) In vivo effects of a GPR30 antagonist. *Nature Chemical Biology*. [Online] 5 (6), 421–427. Available from: doi:10.1038/nchembio.168.
- Dennis, M.K., Field, A.S., Burai, R., Ramesh, C., et al. (2011) Identification of a GPER/GPR30 antagonist with improved estrogen receptor counterselectivity. *The Journal of steroid biochemistry and molecular biology*. [Online] 127 (3–5), 358–366. Available from: doi:10.1016/j.jsbmb.2011.07.002.
- Docherty, J.R., Stanford, S.C., Panattieri, R.A., Alexander, S.P.H., et al. (2019) Sex: A change in our guidelines to authors to ensure that this is no longer an ignored experimental variable. *British Journal of Pharmacology*. [Online] 176 (21), 4081–4086. Available from: doi:10.1111/bph.14761.
- Ferreira, N.S., Cau, S.B.A., Silva, M.A.B., Manzato, C.P., et al. (2015) Diabetes impairs the vascular effects of aldosterone mediated by G protein-coupled

estrogen receptor activation. *Frontiers in Pharmacology*. 6, 34.

Ficker, E. (2003) Role of the Cytosolic Chaperones Hsp70 and Hsp90 in Maturation of the Cardiac Potassium Channel hERG. *Circulation Research*. [Online] Available from: doi:10.1161/01.RES.0000079028.31393.15.

Filardo, E.J., Quinn, J.A., Bland, K.I. & Frackelton, A.R.J. (2000) Estrogen-induced activation of Erk-1 and Erk-2 requires the G protein-coupled receptor homolog, GPR30, and occurs via trans-activation of the epidermal growth factor receptor through release of HB-EGF. *Molecular endocrinology (Baltimore, Md.)*. [Online] 14 (10), 1649–1660. Available from: doi:10.1210/mend.14.10.0532.

Gao, Y., Yechikov, S., Vazquez, A.E., Chen, D., et al. (2013) Distinct Roles of Molecular Chaperones HSP90 $\alpha$  and HSP90 $\beta$  in the Biogenesis of KCNQ4 Channels. *PLoS ONE*. [Online] Available from: doi:10.1371/journal.pone.0057282.

Haavisto, A.M., Pettersson, K., Bergendahl, M., Perheentupa, A., et al. (1993) A supersensitive immunofluorometric assay for rat luteinizing hormone. *Endocrinology*. [Online] Available from: doi:10.1210/endo.132.4.8462469.

Hulley, S., Furberg, C., Barrett-Connor, E., Cauley, J., et al. (2002) Noncardiovascular disease outcomes during 6.8 years of hormone therapy: Heart and Estrogen/progestin Replacement Study follow-up (HERS II). *Journal of the American Medical Association*. [Online] Available from: doi:10.1001/jama.288.1.58.

Hulley, S., Grady, D., Bush, T., Furberg, C., et al. (1998) Randomized trial of estrogen plus progestin for secondary prevention of coronary heart disease in postmenopausal women. Heart and Estrogen/progestin Replacement Study (HERS) Research Group. *JAMA*. [Online] 280 (7), 605–613. Available from:

doi:10.1001/jama.280.7.605.

Jaimes, L., Vinet, R., Knox, M., Morales, B., et al. (2019) A Review of the Actions of Endogenous and Exogenous Vasoactive Substances during the Estrous Cycle and Pregnancy in Rats. *Animals: an open access journal from MDPI*. [Online] 9 (6). Available from: doi:10.3390/ani9060288.

Jepps, T.A., Bentzen, B.H., Stott, J.B., Povstyan, O. V., et al. (2014) Vasorelaxant effects of novel Kv7.4 channel enhancers ML213 and NS15370. *British Journal of Pharmacology*. [Online] 171 (19), 4413–4424. Available from: doi:10.1111/bph.12805.

Jepps, T.A., Chadha, P.S., Davis, A.J., Harhun, M.I., et al. (2011) Downregulation of Kv7.4 channel activity in primary and secondary hypertension. *Circulation*. [Online] Available from: doi:10.1161/CIRCULATIONAHA.111.032136.

Kow, L.-M. & Pfaff, D.W. (2016) Rapid estrogen actions on ion channels: A survey in search for mechanisms. *Steroids*. [Online] 111, 46–53. Available from: doi:10.1016/j.steroids.2016.02.018.

Mackie, A.R., Brueggemann, L.I., Henderson, K.K., Shiels, A.J., et al. (2008) Vascular KCNQ potassium channels as novel targets for the control of mesenteric artery constriction by vasopressin, based on studies in single cells, pressurized arteries, and in vivo measurements of mesenteric vascular resistance. *Journal of Pharmacology and Experimental Therapeutics*. [Online] Available from: doi:10.1124/jpet.107.135764.

Maiti, K., Paul, J.W., Read, M., Chan, E.C., et al. (2011) G-1-activated membrane estrogen receptors mediate increased contractility of the human myometrium. *Endocrinology*. [Online] 152 (6), 2448–2455. Available from: doi:10.1210/en.2010-0979.



- Mazzuca, M.Q., Mata, K.M., Li, W., Rangan, S.S., et al. (2015) Estrogen receptor subtypes mediate distinct microvascular dilation and reduction in  $[Ca^{2+}]_i$  in mesenteric microvessels of female rat. *The Journal of pharmacology and experimental therapeutics*. [Online] 352 (2), 291–304. Available from: doi:10.1124/jpet.114.219865.
- Möller, C. & Netzer, R. (2006) Effects of estradiol on cardiac ion channel currents. *European journal of pharmacology*. [Online] 532 (1–2), 44–49. Available from: doi:10.1016/j.ejphar.2006.01.006.
- Mondéjar-Parreño, G., Moral-Sanz, J., Barreira, B., De la Cruz, A., et al. (2019) Activation of Kv7 channels as a novel mechanism for NO/cGMP-induced pulmonary vasodilation. *British Journal of Pharmacology*. [Online] Available from: doi:10.1111/bph.14662.
- Mulvany, M.J. & Halpern, W. (1976) Mechanical properties of vascular smooth muscle cells in situ. *Nature*. [Online] 260 (5552), 617–619. Available from: doi:10.1038/260617a0.
- Ng, F.L., Davis, A.J., Jepps, T.A., Harhun, M.I., et al. (2011) Expression and function of the K<sup>+</sup> channel KCNQ genes in human arteries. *British Journal of Pharmacology*. [Online] 162 (1), 42–53. Available from: doi:10.1111/j.1476-5381.2010.01027.x.
- Nilsson, M.E., Vandenput, L., Tivesten, Å., Norlén, A.-K., et al. (2015) Measurement of a Comprehensive Sex Steroid Profile in Rodent Serum by High-Sensitive Gas Chromatography-Tandem Mass Spectrometry. *Endocrinology*. [Online] 156 (7), 2492–2502. Available from: doi:10.1210/en.2014-1890.
- Novella, S., Pérez-Cremades, D., Mompeón, A. & Hermenegildo, C. (2019) Mechanisms underlying the influence of oestrogen on cardiovascular physiology

- in women. *Journal of Physiology*. [Online] 597 (19), 4873–4886. Available from: doi:10.1113/JP278063.
- O'Mahony, F., Alzamora, R., Betts, V., LaPaix, F., et al. (2007) Female gender-specific inhibition of KCNQ1 channels and chloride secretion by 17 $\beta$ -estradiol in rat distal colonic crypts. *Journal of Biological Chemistry*. [Online] Available from: doi:10.1074/jbc.M611682200.
- O'Mahony, F., Alzamora, R., Chung, H.-L., Thomas, W., et al. (2009) Genomic priming of the antisecretory response to estrogen in rat distal colon throughout the estrous cycle. *Molecular endocrinology (Baltimore, Md.)*. [Online] 23 (11), 1885–1899. Available from: doi:10.1210/me.2008-0248.
- Ohya, S., Sergeant, G.P., Greenwood, I.A. & Horowitz, B. (2003) Molecular variants of KCNQ channels expressed in murine portal vein myocytes: A role in delayed rectifier current. *Circulation Research*. [Online] Available from: doi:10.1161/01.RES.0000070880.20955.F4.
- Pabbidi, M.R., Kuppusamy, M., Didion, S.P., Sanapureddy, P., et al. (2018) Sex differences in the vascular function and related mechanisms: role of 17 $\beta$ -estradiol. *American Journal of Physiology-Heart and Circulatory Physiology*. [Online] 315 (6), H1499–H1518. Available from: doi:10.1152/ajpheart.00194.2018.
- Rapetti-Mauss, R., O'Mahony, F., Sepulveda, F. V., Urbach, V., et al. (2013) Oestrogen promotes KCNQ1 potassium channel endocytosis and postendocytic trafficking in colonic epithelium. *Journal of Physiology*. [Online] Available from: doi:10.1113/jphysiol.2013.251678.
- Roepke, T.A., Qiu, J., Smith, A.W., Ronnekleiv, O.K., et al. (2011) Fasting and 17 $\beta$ -estradiol differentially modulate the M-current in neuropeptide Y neurons. *Journal of Neuroscience*. [Online] 31 (33), 11825–11835. Available from:

doi:10.1523/JNEUROSCI.1395-11.2011.

Schnee, M.E. & Brown, B.S. (1998) Selectivity of linopirdine (DuP 996), a neurotransmitter release enhancer, in blocking voltage-dependent and calcium-activated potassium currents in hippocampal neurons. *Journal of Pharmacology and Experimental Therapeutics*.

Simoncini, T., Hafezi-Moghadam, A., Brazil, D.P., Ley, K., et al. (2000) Interaction of oestrogen receptor with the regulatory subunit of phosphatidylinositol-3-OH kinase. *Nature*. [Online] 407 (6803), 538–541. Available from: doi:10.1038/35035131.

Stott, J.B., Barrese, V., Jepps, T.A., Leighton, E. V., et al. (2015) Contribution of Kv7 channels to natriuretic peptide mediated vasodilation in normal and hypertensive rats. *Hypertension*. [Online] 65 (3), 676–682. Available from: doi:10.1161/HYPERTENSIONAHA.114.04373.

Stricker, R., Eberhart, R., Chevailler, M.-C., Quinn, F.A., et al. (2006) Establishment of detailed reference values for luteinizing hormone, follicle stimulating hormone, estradiol, and progesterone during different phases of the menstrual cycle on the Abbott ARCHITECT analyzer. *Clinical chemistry and laboratory medicine*. [Online] 44 (7), 883–887. Available from: doi:10.1515/CCLM.2006.160.

Takezawa, H., Hayashi, H., Sano, H., Saito, H., et al. (1994) Circadian and estrous cycle-dependent variations in blood pressure and heart rate in female rats. *The American journal of physiology*. [Online] 267 (5 Pt 2), R1250-6. Available from: doi:10.1152/ajpregu.1994.267.5.R1250.

Thomas, G.P., Gerlach, U. & Antzelevitch, C. (2003) HMR 1556, a potent and selective blocker of slowly activating delayed rectifier potassium current. *Journal of Cardiovascular Pharmacology*. [Online] Available from: doi:10.1097/00005344-

200301000-00018.

Yan, F.-F., Pratt, E.B., Chen, P.-C., Wang, F., et al. (2010) Role of Hsp90 in biogenesis of the beta-cell ATP-sensitive potassium channel complex. *Molecular biology of the cell*. [Online] 21 (12), 1945–1954. Available from: doi:10.1091/mbc.e10-02-0116.

Yang, X.-P. & Reckelhoff, J.F. (2011) Estrogen, hormonal replacement therapy and cardiovascular disease. *Current opinion in nephrology and hypertension*. [Online] 20 (2), 133–138. Available from: doi:10.1097/MNH.0b013e3283431921.

Yeung, S.Y.M., Pucovský, V., Moffatt, J.D., Saldanha, L., et al. (2007) Molecular expression and pharmacological identification of a role for Kv7 channels in murine vascular reactivity. *British Journal of Pharmacology*. [Online] 151 (6), 758–770. Available from: doi:10.1038/sj.bjp.0707284.

Accepted Article

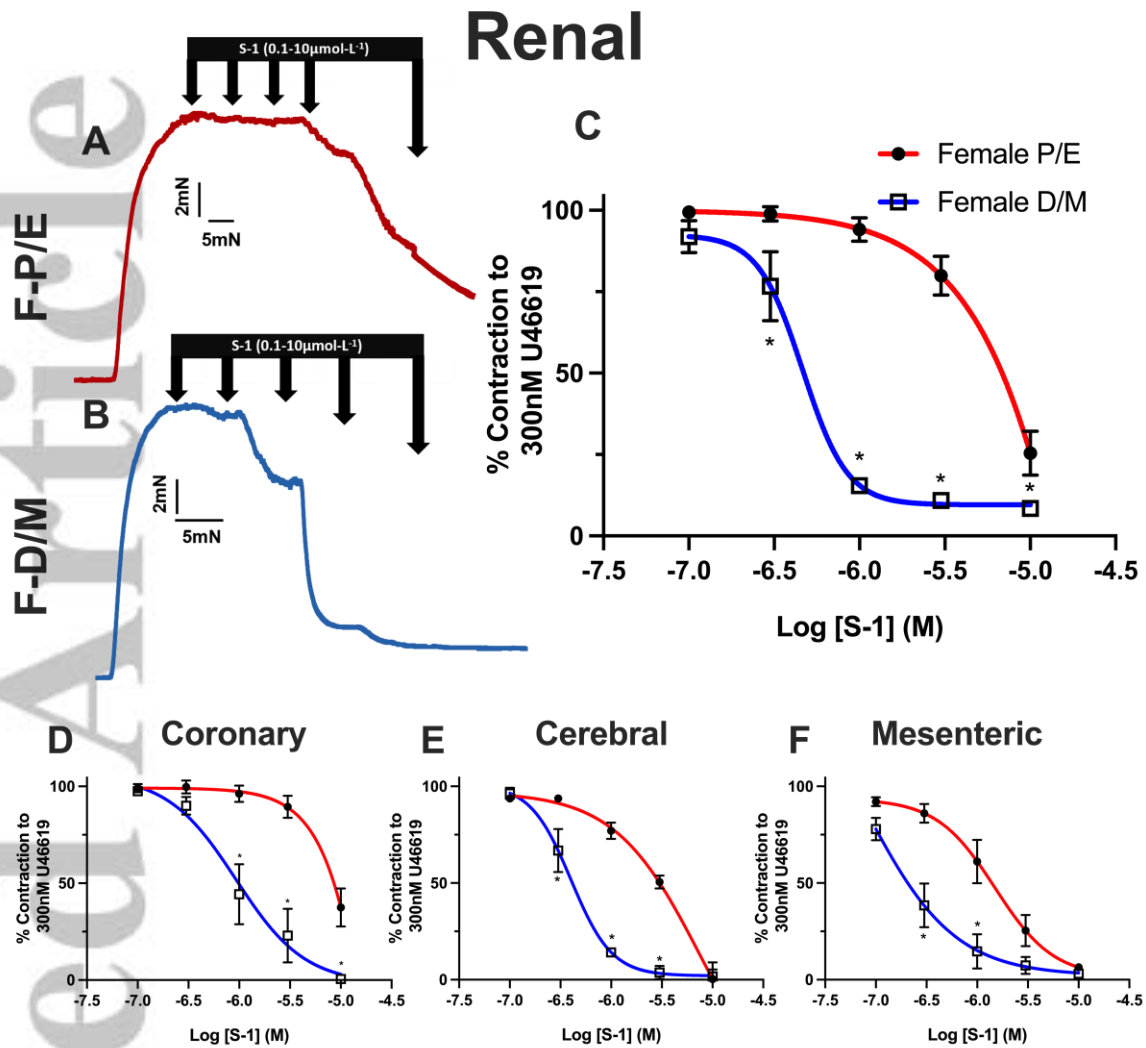


Figure 1: Oestrus cycle dependent differences in S-1 mediated relaxation of pre-contracted tone within arteries from female (P/E2) and female (D/M) Wistar rats.

Representative traces of relaxation of pre-contracted arterial tone (U46619; 300nmol-L<sup>-1</sup>) in renal arteries from female pro-oestrus/oestrus (P/E; red; A) and female di-oestrus/met-oestrus (D/M; blue; B) in response to Kv7.2-5 activator S-1 (0.1-10µmol-L<sup>-1</sup>). Mean data of S-1 mediated relaxation in renal ( $n=5-8$ ; C), coronary ( $n=4-8$ ; D), cerebral ( $n=5-7$ ; E) and mesenteric ( $n=5-6$ ; F) arteries. Values are expressed as means  $\pm$  SEM error bars (C-F). A two-way statistical ANOVA with a post-hoc Bonferroni test was used to generate significance values (\*=  $P \leq 0.05$ ). ( $n$ ) number of animals.

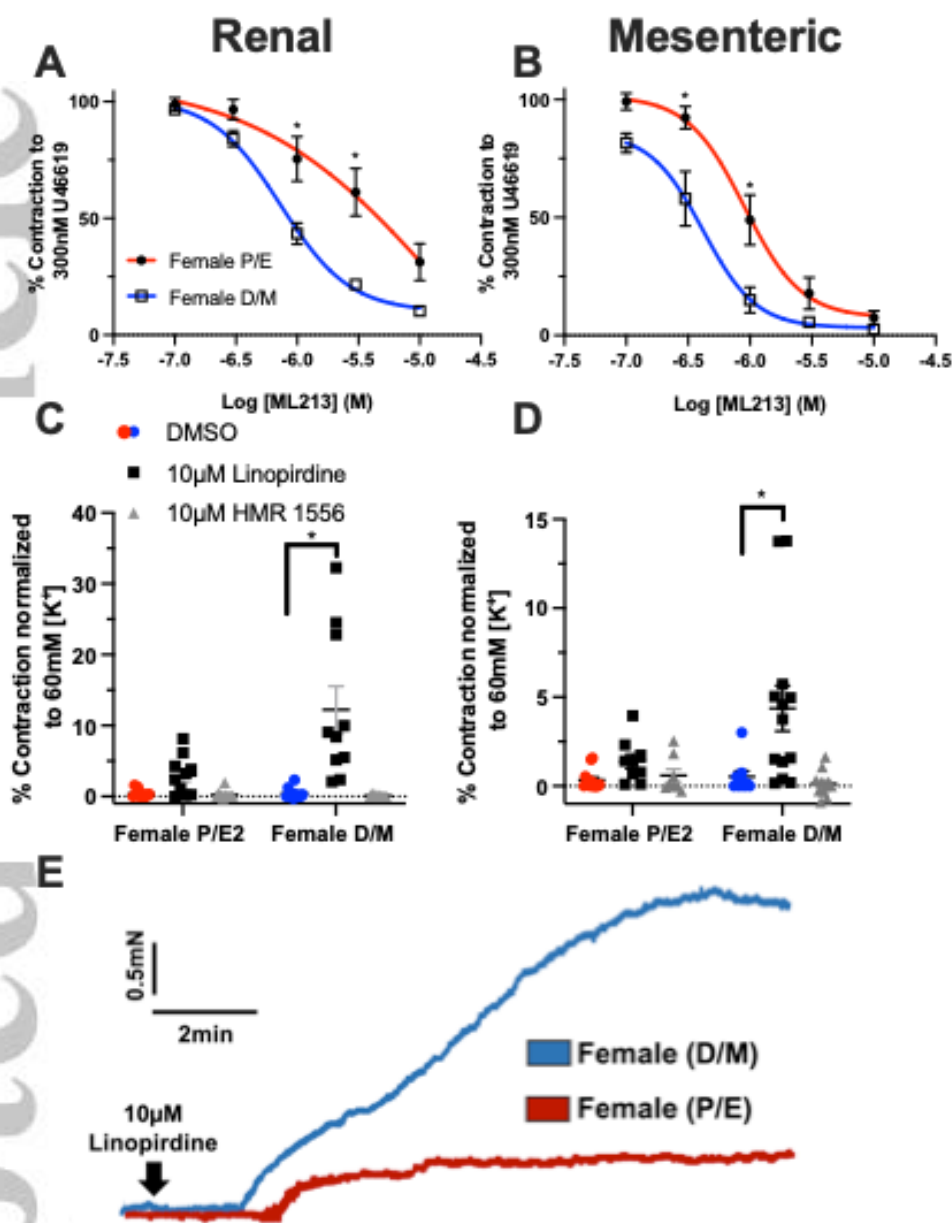


Figure 2:  $K_v7$  channel modulators are more efficacious and potent in arteries from female (D/M) Wistar rats when compared to female (P/E) rats.

Mean data of relaxation of pre-contracted tone (U46619;  $300\text{nmol}\cdot\text{L}^{-1}$ ) in response to ML213 ( $0.01\text{-}10\mu\text{mol}\cdot\text{L}^{-1}$ ) in renal ( $n=5\text{-}6$ ; A) and mesenteric ( $n=5\text{-}6$ ; B) arteries from female pro-oestrus/oestrus (P/E; red) and female di-oestrus/met-oestrus (D/M; blue) rats. Mean data of increases in basal tone in response to solvent control DMSO (Female P/E, red; Female D/M, blue), Linopirdine ( $10\mu\text{mol}\cdot\text{L}^{-1}$ ; black) and HMR-1556 ( $10\mu\text{mol}\cdot\text{L}^{-1}$ ; grey) in renal ( $n=10\text{-}12$ ; C) and mesenteric arteries ( $n=10\text{-}13$ ; D). Representative traces of contraction of renal arteries from female P/E (red) and female D/M (blue) rats in response to pan  $K_v7$  channel blocker Linopirdine ( $10\mu\text{mol}\cdot\text{L}^{-1}$ ; E). All values are expressed as means  $\pm$  SEM error bars. A two-way statistical ANOVA with a post-hoc Bonferoni (A,B) or Dunnet (C,D) correction was used to generate significance values ( $*=P\leq 0.05$ ; B/E). ( $n=$ ) number of animals.

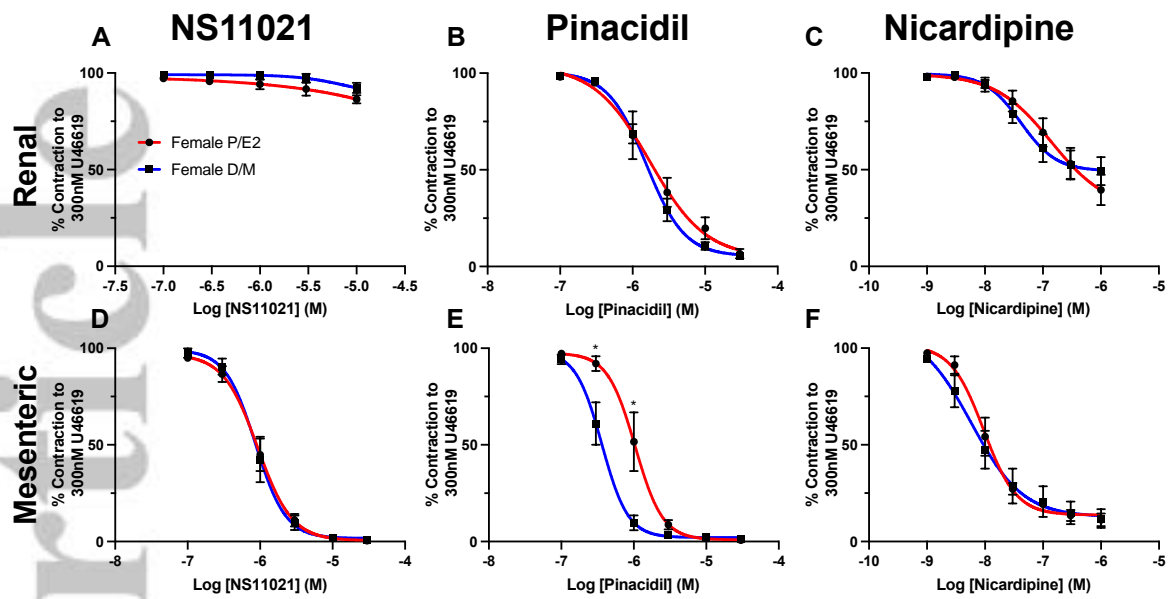


Figure 3: Effect of different ion channel modulators in renal arteries from female (P/E) and female (D/M) Wistar rats.

NS11021 ( $0.1-30\mu\text{mol}\cdot\text{L}^{-1}$ ; A,D), pinacidil ( $0.1-30\mu\text{mol}\cdot\text{L}^{-1}$ ; B,E) and nicardipine ( $0.001-1\mu\text{mol}\cdot\text{L}^{-1}$ ; C,F) mediated relaxation of pre-constricted arterial tone ( $300\text{nmol}\cdot\text{L}^{-1}$  U46619) in renal (A-C) and mesenteric (D-F) arteries from female pro-oestrus/oestrus (P/E; red;  $n=5$ ) and female di-oestrus/met-oestrus (D/M; blue;  $n=5-7$ ) Wistar rats. All values are expressed as means  $\pm$  SEM error bars. A two-way statistical ANOVA with a post-hoc Bonferroni test was used to generate significance values ( $*=P\leq 0.05$ ). ( $n=$ ) number of animals used (A-F).

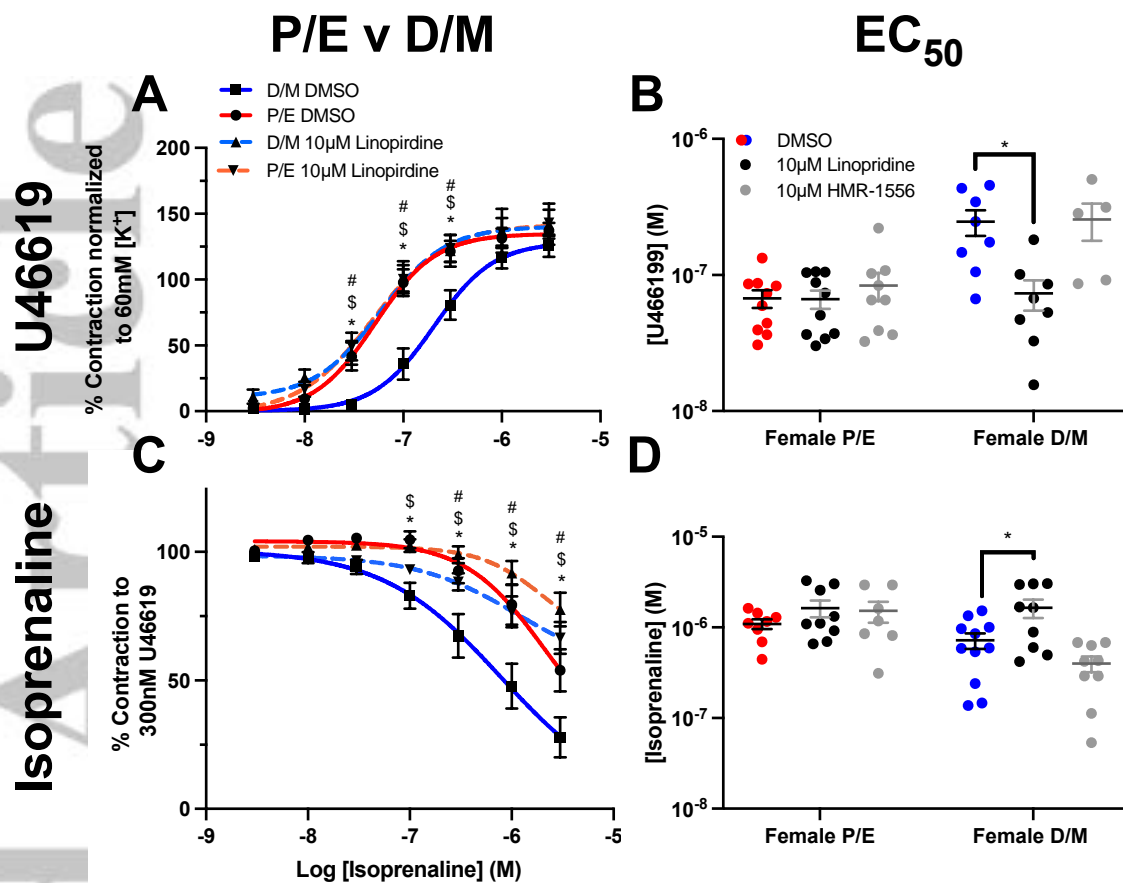


Figure 4: Linopirdine alters receptor mediated responses in renal arteries from female D/M, but not female P/E Wistars.

Mean data of contraction in response to U46619 ( $0.003\text{-}3\ \mu\text{mol-L}^{-1}$ ;  $n=7\text{-}10$ ; A) and relaxation of pre-contracted arterial tone ( $300\ \text{nmol-L}^{-1}$  U46619) in response to isoprenaline ( $0.003\text{-}3\ \mu\text{mol-L}^{-1}$ ;  $n=9\text{-}10$ ; C) within renal arteries preincubated within DMSO solvent control (Female di-oestrus/met-oestrus (D/M), blue; Female pro-oestrus/oestrus (P/E), red) or Linopirdine ( $10\ \mu\text{mol-L}^{-1}$ ; Female D/M, blue-dashed line; Female P/E, red-dashed line). Scatter graph representing the raw  $EC_{50}$  values of U46619 mediated contraction (B) or isoprenaline mediated relaxation (D) within renal arteries of the mean data to the left, in addition to vessels pre-incubated in Kv7.1 specific blocker HMR-1556 ( $10\ \mu\text{mol-L}^{-1}$ ; grey). A two-way statistical ANOVA with a post-hoc Bonferroni (A,C) or Dunnet (B,D) correction was used to generate significance values; values (\*/#/\$  $P\leq 0.05$ ; \*= D/M DMSO v P/E DMSO; # = D/M DMSO v D/M  $10\ \mu\text{mol-L}^{-1}$  Linopirdine; \$ = D/M DMSO v P/E  $10\ \mu\text{mol-L}^{-1}$  Linopirdine; \* = condition v DMSO solvent control, C,D) ( $n=$ ) number of animals used (A-D).



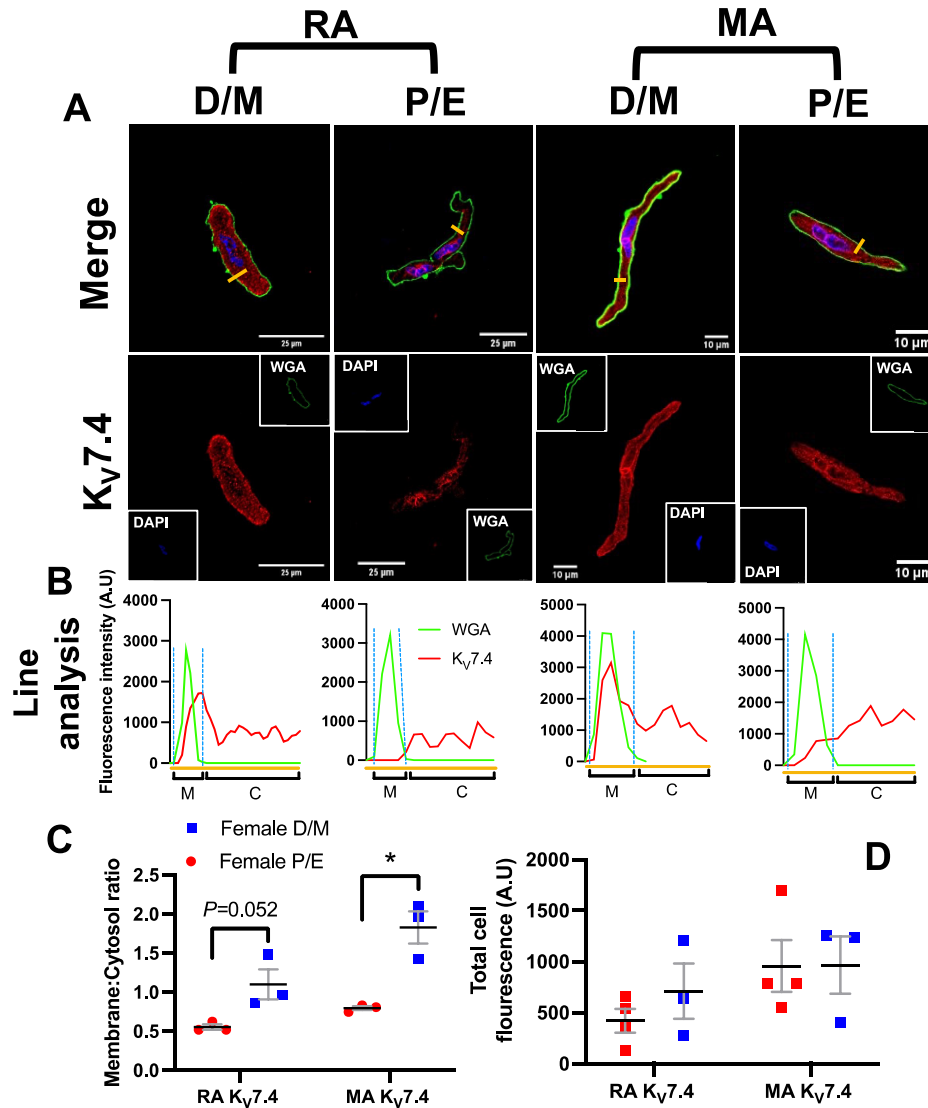


Figure 5: Oestrus cycle-dependent reduction in Kv7.4 subcellular distribution in mesenteric and renal artery myocytes.

Representative images of immunocytochemistry demonstrates Kv7.4 expression (red) within renal (RA) and mesenteric (MA; A) artery vascular smooth muscle cells from female di-oestrus/met-oestrus (D/M;  $n=3$ ) and female pro-oestrus/oestrus (P/E;  $n=3$ ) Wistar rats. Plasma membrane and nuclear markers, wheat germ agglutinin (WGA; green) and 4',6-diamidino-2-phenylindole (DAPI; blue) respectively, are also shown. Fluorescence intensity profiles were plotted for Kv7.4 and WGA measured in arbitrary units (A.U) along the yellow line seen in the merged image above (B). Fluorescence intensity  $\geq 200$  A.U was considered as the plasma membrane (M) and below the threshold was considered as the cytosol (C; B). Bar chart demonstrating mean data of the Membrane:Cytosol ratio for Kv7.4 expression in P/E and D/M RA and MA (C). Membrane:Cytosol ratio for Kv7.4 expression was calculated by measuring the fluorescence intensity of Kv7.4 within the membrane and dividing it by the fluorescence intensity of Kv7.4 within cytosol from three randomly drawn lines in 10-12 cells pre  $n$ . Mean data for total cell fluorescence (A.U; D). All values are expressed as means  $\pm$  SEM error bars. A 2-way statistical ANOVA with a post-hoc Bonferroni correction was used to generate significance values. ( $n=$ ) number of animals used.

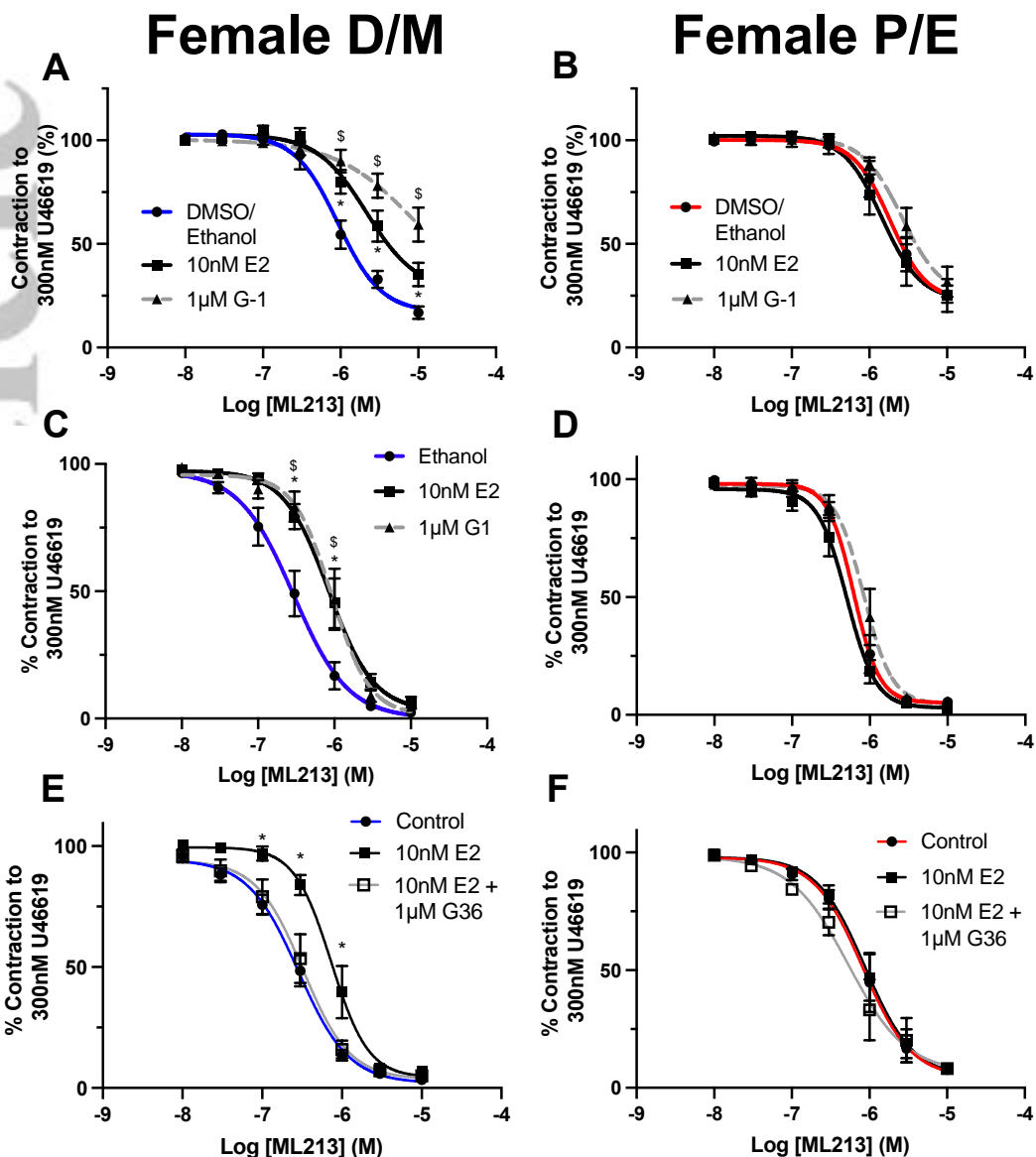


Figure 6: Oestradiol E2 attenuation of ML213 is GPER1 mediated.

Mean data for ML213 mediated relaxation of pre-constricted arterial tone (U46619; 300 nmol-L<sup>-1</sup>) in renal (A,B) and mesenteric (C-F) arteries from female Wistar rats in di-oestrus/met-oestrus (F-D/M; A,B,C; *n*=5-12) or pro-oestrus/oestrus (F-P/E; D,E,F; *n*=6-11) pre-incubated in the DMSO/Ethanol solvent control (F-D/M, blue; F-P/E, red), Oestradiol (E2; 10 nmol-L<sup>-1</sup>; black) or GPER1 agonist G-1 (1 µmol-L<sup>-1</sup>; grey; A-D) or GPER1 antagonist G36 (1 µmol-L<sup>-1</sup>) in combination with E2 (10 nmol-L<sup>-1</sup>; grey, hollow square; E,F). All values are expressed as means ± SEM error bars. A two-way statistical ANOVA with a post-hoc Dunnet's test was used to generate significance values (\*/\$=P≤0.05; \*= DMSO/Ethanol v 10nM E2; \$= DMSO/Ethanol v 1µM G-1; A-F). (*n*=) number of animals used (A-F).

## Female D/M

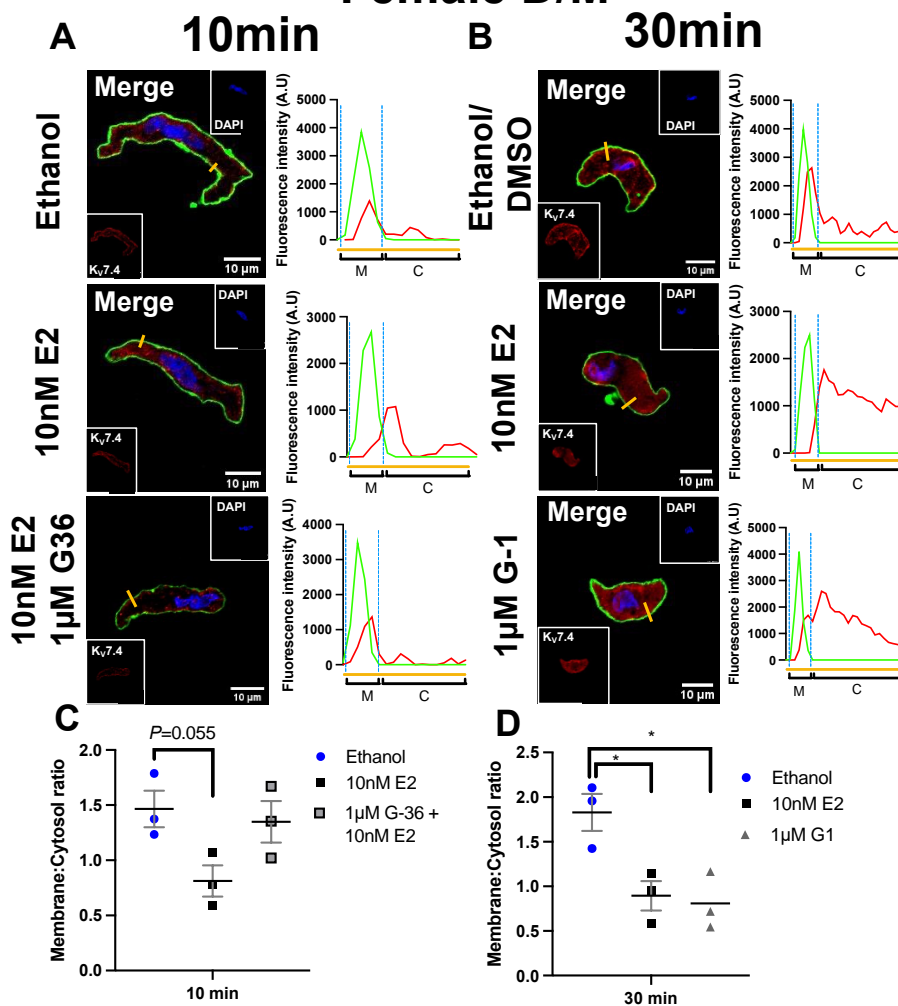


Figure 7: Oestradiol E2 incubation diminishes Kv7.4 membrane abundance in isolated mesenteric artery vascular smooth muscle cells from Female D/M Wistar rats.

Representative images of immunocytochemistry demonstrates Kv7.4 expression (red) from female di-oestrus/met-oestrus (D/M;  $n=3$ ) mesenteric artery vascular smooth muscle cells pre-incubated in either solvent control (ethanol/DMSO), Oestradiol (E2;  $10 \text{ nmol-L}^{-1}$ ) or E2 + GPER1 antagonist G-36 ( $1 \text{ } \mu\text{mol-L}^{-1}$ ) for 10 minutes (A) or (ethanol/DMSO), E2 ( $10 \text{ nmol-L}^{-1}$ ) or GPER1 agonist G-1 ( $1 \text{ } \mu\text{mol-L}^{-1}$ ; B) for 30 minutes (B). Plasma membrane and nuclear markers wheat germ agglutinin (WGA; green) and 4',6-diamidino-2-phenylindole (DAPI; blue) are also shown. Fluorescence intensity profiles were plotted for Kv7.4 and WGA measured in arbitrary units (A.U) along the yellow line seen in the merged image above. Fluorescence intensity  $\geq 200$  A.U was considered the plasma membrane (M) and below the threshold was considered the cytosol. Bar chart demonstrating mean data of the Membrane:Cytosol ratio for Kv7.4 expression solvent control (blue), E2 (grey) or G-36+E2 / G-1 (grey, square pattern; 10min, C; 30 min, D). Membrane:Cytosol ratio for Kv7.4 expression was calculated by measuring the fluorescence intensity of Kv7.4 within the membrane and dividing it by the fluorescence intensity of Kv7.4 within cytosol from three randomly drawn lines in 10-12 cells pre  $n$ . All values are expressed as means  $\pm$  SEM error bars. A 2-way statistical ANOVA with a post-hoc Dunnet's correction was used to generate significance values. ( $n=$ ) number of animals used.

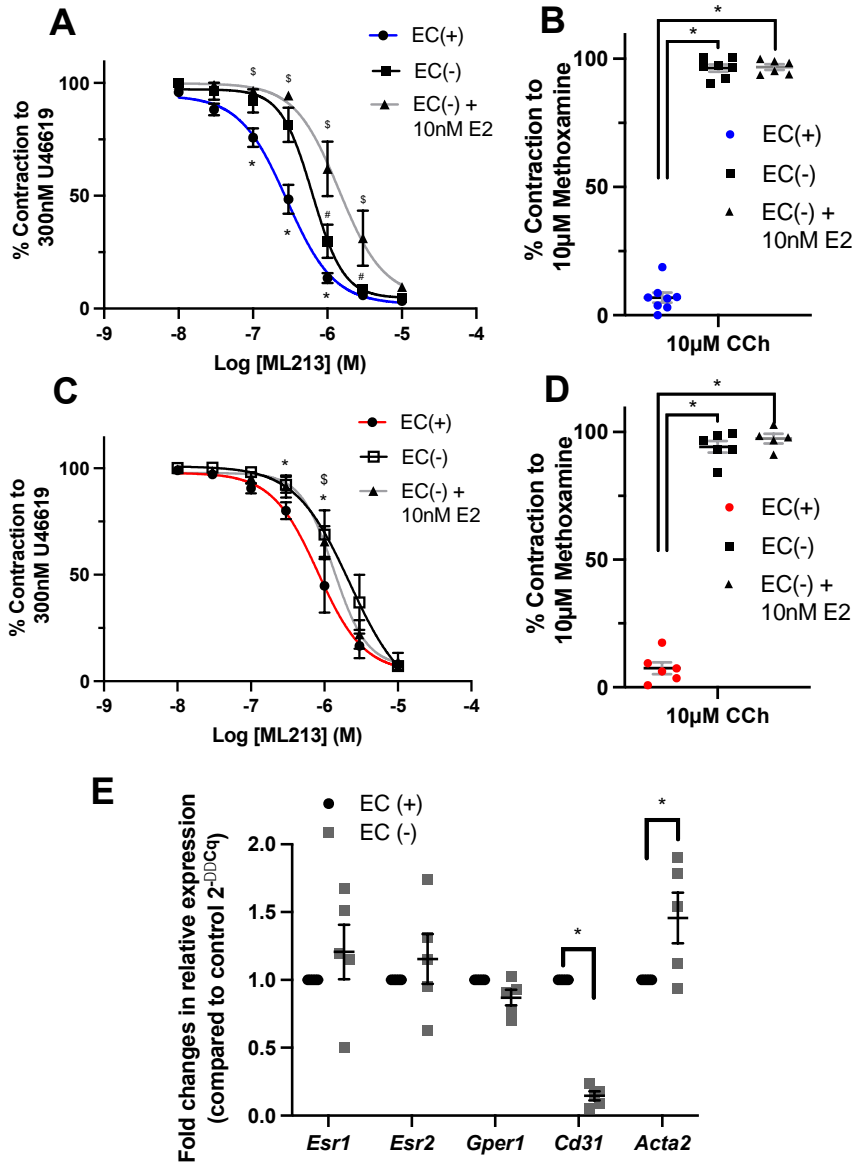


Figure 8: Oestradiol E2 attenuation of ML213 mediated relaxation is not endothelium dependent.

Mean data for ML213 mediated relaxation of pre-constricted arterial tone (U46619; 300 nmol-L<sup>-1</sup>) in arteries from female Wistar rats in di-oestrus/met-oestrus (F-D/M; A,B;  $n=6-8$ ) or pro-oestrus/oestrus (F-P/E; D,E;  $n=5-6$ ) in the presence (F-D/M, blue; F-P/E, red) and absence (black) of endothelial cells (ECs(+)/(-)) and in the absence of endothelial cells pre-incubated in Oestradiol (10 nmol-L<sup>-1</sup>; EC(-) + E2; grey). Mean data and scatter plot for carbachol (CCh) mediated relaxation of pre-contracted arterial tone (methoxamine 10 µmol-L<sup>-1</sup>) generated within the same vessels prior to application of ML213 (B,D). All values are expressed as means  $\pm$  SEM error bars. Relative fold expression in Oestrogen receptors (*Esr1*, 2 and *Gper1*), EC marker *Cd31* and vascular smooth muscle marker *Acta2* in whole lysates of mesenteric arteries from female Wistars within vessels denuded of endothelium (EC (-)) compared with vessels with intact endothelium (EC (+);  $2^{-\Delta\Delta Cq}$ ;  $n=5$ ; E). A two-way statistical ANOVA with a post-hoc Bonferroni test was used to generate significance values (\*/#/\$= $P\leq 0.05$ ). Comparisons include; \*= EC(+) v EC(-), \$= EC(+) v EC(-) + 10nM E2; #= EC(-) v EC(-) + 10nM E2; A-D). ( $n=$ ) number of animals used (A-F).

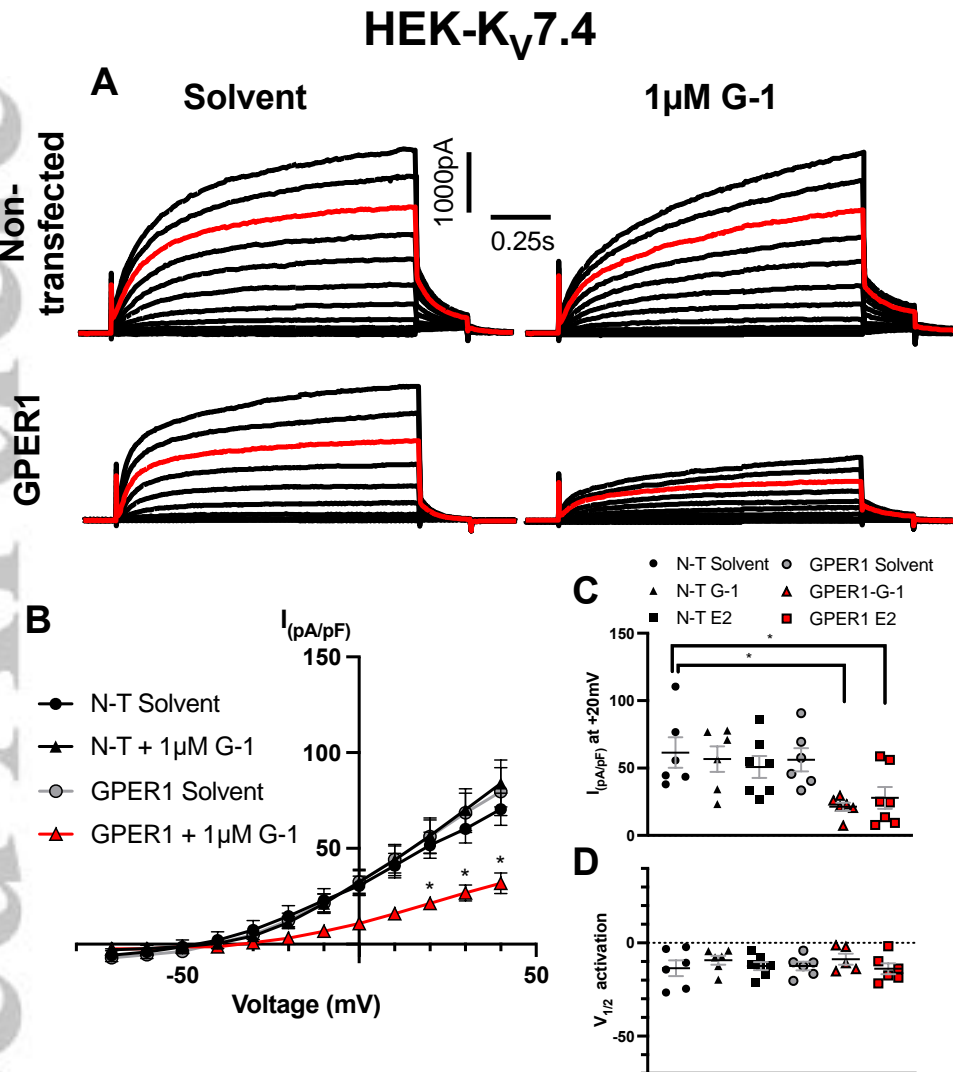


Figure 9: Oestradiol E2 and G1 pre-incubation impairs K<sub>v</sub>7.4 channel activity in GPER1 transfected cells.

Representative current recordings during ruptured whole cell voltage-clamp in non-transfected (NT) HEK- K<sub>v</sub>7.4 pre-incubated (30min) in solvent control (upper left) or G-1 (1µmol·L<sup>-1</sup>; upper right) and GPER1-transfected cells pre-incubated in solvent control (lower left) or G-1 (lower right; A). Red line represents current flow in response to +20mV. Cells were held at a holding potential of -60mV, then stepped to test voltage for 1.5sec every 15 sec ranging from -70mV to +40mV increasing in 10mV intervals. Before returning to rest potential, voltage was stepped to an inactivation potential of -40mV. Mean *IV* relationships plotted for HEK- K<sub>v</sub>7.4 cells; NT in solvent control (black, circle; *n*= 5) or G-1 (black, triangle; *n*= 6) and GPER1 transfected cells in solvent (grey, circle; DMSO; *n*= 6) or G-1 (red, triangle; red; *n*= 6; B). Scatter graph demonstrates peak current amplitude at +20mV in non-transfected cells pre-incubated in solvent control (black, circle; *n*=6), G-1 (black triangle; *n*=6), Oestradiol E2 (10 nmol·L<sup>-1</sup>; black, square; *n*=7) and GPER1 transfected cells solvent control (grey, circle; *n*=6), G-1 (red triangle; *n*=6), Oestradiol E2 (red, square; *n*=7; C). Voltage dependence of activation for K<sub>v</sub>7.4 currents (D). All values are expressed as means ± SEM error bars. A 2-way statistical ANOVA (B) with a post-hoc Dunnet's correction or a 1-way statistical ANOVA (C,D) was used to generate significance values. (\*= *P*≤0.05) condition vs non-transfected solvent control. (*n*=) number of animals used.

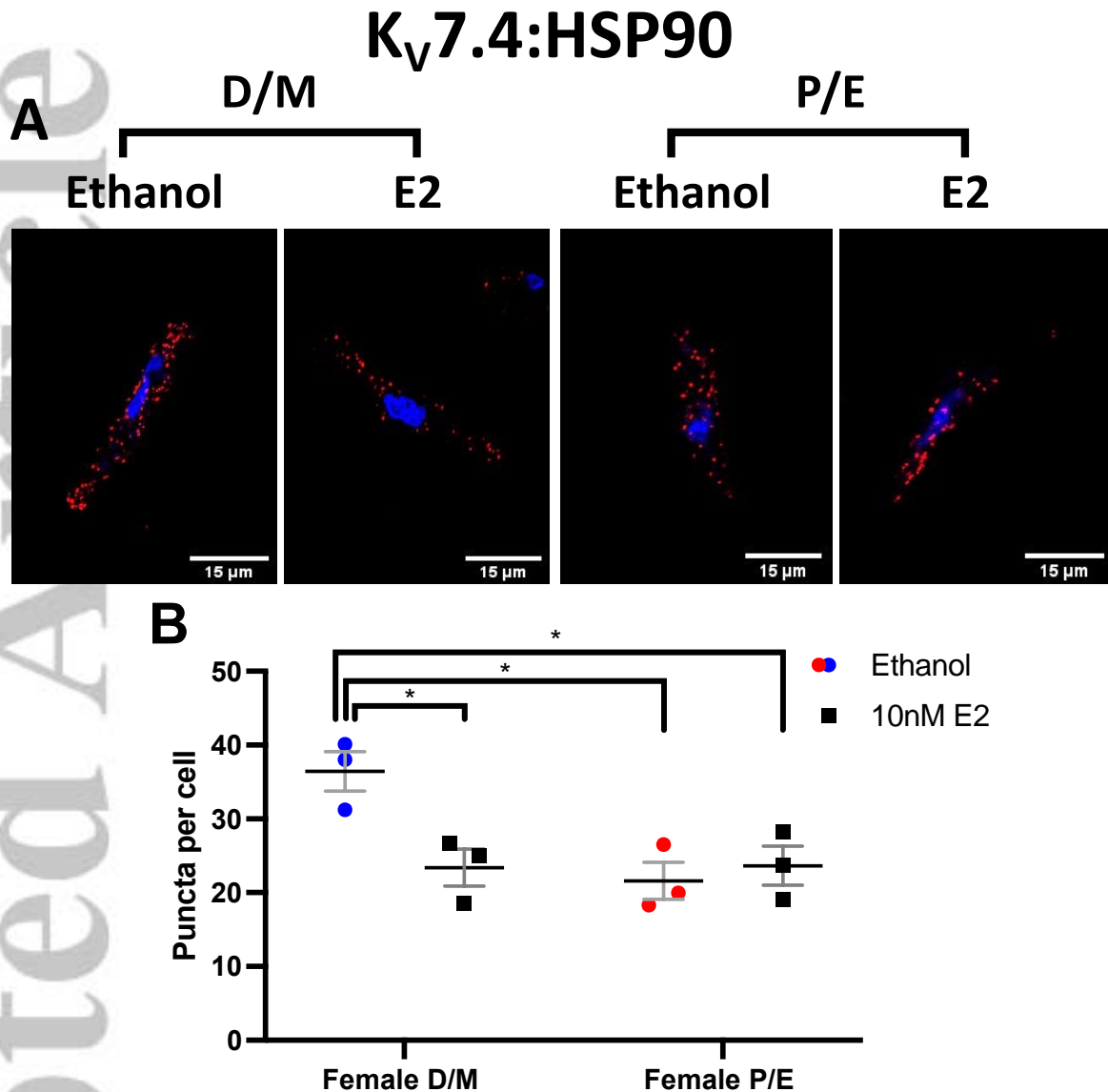


Figure 10: Oestradiol reduces K<sub>v</sub>7.4-Heat shock protein 90 interactions in F-D/M, but not F-P/E mesenteric artery myocytes.

Proximity ligation assay (PLA) for K<sub>v</sub>7.4 and Heat shock protein 90 (HSP90) interaction within female di-oestrus/met-oestrus (D/M) and female pro-oestrus/oestrus (P/E) mesenteric artery myocytes pre-incubated in either ethanol or 10nmol-L<sup>-1</sup> Oestradiol E2 (E2; 30min; *n*=3). Representative images of mesenteric artery myocyte mid-cell cross section exhibit fluorescent puncta which illustrate K<sub>v</sub>7.4:HSP90 interactions within a distance of <40nm (red) and the nucleoli via 4',6-diamidino-2-phenylindole (DAPI; blue). Bar graph of mean data for puncta per cell in an xy cross section. All values are expressed as mean ± SEM. A 2-way statistical ANOVA with a post-hoc Dunnet's correction was used to generate significance values. (*n*=) number of animals used, 10-15 cells per *n*.

Table 1: RT-qPCR primers

<b>Gene</b>	<b>(+) Forward primer sequence</b> <b>(-) Reverse primer sequence</b>	<b>Gene accession number</b>	<b>Amplicon (bp)</b>
<b>Kcnq1</b>	TGGGTCTCATCTTCTCCTCC GTAGCCAATGGTGGTGACTG	NM_032073	124
<b>Kcnq2</b>	AAGAGCAGCATCGGCAAAAA GGTGCGTGAGAGGTTAGTAGCA	NM_133322	101
<b>Kcnq3</b>	CAGCAAAGAACTCATCACCG ATGGTGGCCAGTGTGATCAG	AF091247	161
<b>Kcnq4</b>	GAATGAGCAGCTCCCAGAAG AAGCTCCAGCTTTTCTGCAC	XM_233477.8	133
<b>Kcnq5</b>	AACTGATGAGGAGGTCCGGTG GATGACCGTGACCTTCCAGT	XM_001071249.3	120
<b>Kcne1</b>	GTTTCCCCAAATCTCTCCATT AGCACACACTTCCCATTTCOA	NM_008424.3	111
<b>Kcne2</b>	CCTGGTATTTAACTGAGTTGGACAT GCACTGGGGGCTCTTGAAT	NM_133603.2	97
<b>Kcne3</b>	CTCAACCATATCAAGCCACAGT GCCTATCAGTCCCTCTTCTCT	NM_022235.2	99
<b>Kcne4</b>	GGAGGAGGGGGCTGATGA CTGGTGGATGTTCTCGGAAGA	NM_212526.1	88
<b>Kcne5</b>	GCACGAAGAGACCTCAGACAT GGACAGGAAACAAGAACCACAT	NM_001101003.1	146

<b><i>Esr1</i></b>	TTCACCTTCTGGAGTGTGCC ACTTGACGTAGCCAGCAACA	<u>NM_012689.1</u>	173
<b><i>Esr2</i></b>	TGCCGACTTCGCAAGTGTTA ACCGTTTCTCTTGGCTTTGC	NM_012754.2	138
<b><i>Gper1</i></b>	TCATCGGCCTGTGCTATTCC GAAGACAAGGACCACTGCGA	NM_133573	119
<b><i>Cd31</i></b>	CTCCTAAGAGCAAAGAGCAACTTC TACACTGGTATTCCATGTCTCTGG	NM_031591.1	100
<b><i>Acta2</i></b>	ATCCGATAGAACACGGCATC AGGCATAGAGGGACAGCACA	NM_031004.2	228

Accepted



Table 2: Serum hormone concentrations

<b>Hormone</b>	<b>F-P/E</b>			<b>F-D/M</b>			<b>Student's t-test</b>
	<b>Serum concentration (ng/mL)</b>	<b>SEM (±)</b>	<b>(n)</b>	<b>Serum concentration (ng/mL)</b>	<b>SEM</b>	<b>(n)</b>	
<b>Oestradiol</b>	0.36	0.005	8	0.019	0.005	8	*
<b>Testosterone</b>	0.04	0.018	8	0.023	0.005	8	<i>ns</i>
<b>Androstenedione</b>	0.101	0.42	8	0.063	0.015	8	<i>ns</i>
<b>Progesterone</b>	2.977	0.28	6	5.802	1.217	6	*
<b>Aldosterone</b>	0.018	0.006	8	0.017	0.004	8	<i>ns</i>
<b>Follicular stimulating hormone</b>	0.972	0.174	14	0.958	0.274	14	<i>ns</i>
<b>Luteinizing hormone</b>	3.499	0.655	14	3.373	0.368	14	<i>ns</i>

Hormonal serum concentrations was determined via liquid chromatography tandem mass spectrometry (steroids) and ELISA (LH, FSH) and expressed as ng/mL in female rats during either pro-oestrus/oestrus (F-P/E) or di-oestrus/met-oestrus (F-D/M). Results include SEM and number of animals used (*n*). Student's t-test was used to generate significance values, \*= $P \leq 0.05$ .

Accepted